2004-12

Detecting near-UV and near-IR wavelengths with the FOVEON image sensor

Cheak, Seck Fai

Monterey California. Naval Postgraduate School

NAVAL POSTGRADUATE SCHOOL

MONTEREY, CALIFORNIA

THESIS

DETECTING NEAR-UV AND NEAR-IR WAVELENGTHS WITH THE FOVEON IMAGE SENSOR

by

Cheak Seck Fai

December 2004

Thesis Advisor :	Gamani Karunasiri
Co-Advisor :	Richard C. Olsen

Approved for public release: distribution is unlimited

THIS PAGE IS INTENTIONALLY LEFT BLANK.

REPORT DOCUMENTATION PAGE			Form Approved OMB No.
Public reporting burden for this collection of information is estimated to average 1 hour per response, including the time for reviewing instruction, searching existing data sources, gathering and maintaining the data needed, and completing and reviewing the collection of information. Send comments regarding this burden estimate or any other aspect of this collection of information, including suggestions for reducing this burden, to Washington headquarters Services, Directorate for Information Operations and Reports, 1215 Jefferson Davis Highway, Suite 1204, Arlington, VA 22202-4302, and to the Office of Management and Budget, Paperwork Reduction Project (0704-0188) Washington DC 20503.			
1. AGENCY USE ONLY ***(Leave blank)***	**2. REPORT DATE** December 2004	**3. REPORT TYPE AND DATES COVERED** Master's Thesis	
4. TITLE AND SUBTITLE: Title (Mix case letters) Detecting Near-UV and Near-IR Wavelengths with the FOVEON Image Sensor.			**5. FUNDING NUMBERS**
6. AUTHOR(S) Seck Fai, Cheak, MAJ, Singapore Armed Forces			
7. PERFORMING ORGANIZATION NAME(S) AND ADDRESS(ES) Naval Postgraduate School Monterey, CA 93943-5000			**8. PERFORMING ORGANIZATION REPORT NUMBER**
9. SPONSORING / MONITORING AGENCY NAME(S) AND ADDRESS(ES) N/A			**10. SPONSORING / MONITORING AGENCY REPORT NUMBER**
11. SUPPLEMENTARY NOTES The views expressed in this thesis are those of the authors and do not reflect the official policy or position of any Department of Defense or the U.S. Government.			
12a. DISTRIBUTION / AVAILABILITY STATEMENT Approved for public release : distribution is unlimited.			**12b. DISTRIBUTION CODE**

13. ABSTRACT ***(maximum 200 words)***

Traditionally, digital imaging systems rely on the use of dedicated photodetectors to capture specific wavelengths in the visible spectrum. These photodetectors, which are commonly made of silicon, are arranged as arrays to capture the red, green and blue wavelengths. The signal captured by the individual photodetectors must then be interpolated and integrated to obtain the closest color match and the finest possible resolution with reference to the actual object. The use of spatially separated detectors to sense primary colors reduces the resolution by a factor of three compared to black and white imaging. The FOVEON detector technology greatly improves the color and resolution of the image through its vertically arranged, triple well photodetector. This is achieved by exploiting the variation of absorption coefficient of silicon with wavelength in the visible spectrum. Hence, in a silicon detector, the shorter wavelength (e.g. blue) would be mainly absorbed at a shallow depth. A longer wavelength (e.g. red) would penetrate the material deeper than the shorter wavelengths and be primarily absorbed at a greater depth. By producing a layered silicon detector, all three primary colour wavelengths of red, green and blue can be captured simultaneously. This thesis aims to study the FOVEON camera's ability to image light from the near Infrared (NIR) to the Ultra-Violet (UV) range of the electromagnetic spectrum. The imaged obtained using a set of bandpass filters show that the camera has response both in the UV as well as NIR regions.

14. SUBJECT TERMS: Silicon, Photodetector, FOVEON, CMOS, CCD, Detectivity, Responsivity, Triple-well, Color Perception, Metamerism, Image resolution, Atmospheric absorption, Spectral reflectance, Digital Imaging			**15. NUMBER OF PAGES** 79 **16. PRICE CODE**
17. SECURITY CLASSIFICATION OF REPORT Unclassified	**18. SECURITY CLASSIFICATION OF THIS PAGE** Unclassified	**19. SECURITY CLASSIFICATION OF ABSTRACT** Unclassified	**20. LIMITATION OF ABSTRACT** UL

NSN 7540-01-280-5500 Standard Form 298 (Rev. 2-89)
Prescribed by ANSI Std. 239-18

THIS PAGE IS INTENTIONALLY LEFT BLANK.

Approved for public release: distribution is unlimited

DETECTING NEAR-UV AND NEAR-IR WAVELENGTHS WITH THE FOVEON IMAGE SENSOR

Seck Fai, Cheak
Major, Singapore Armed Forces
BSc (Hons), MEng, University of Manchester, UK, 1999

Submitted in partial fulfillment of the
requirements for the degree of

MASTER OF SCIENCE IN COMBAT SYSTEMS TECHNOLOGY

from the

NAVAL POSTGRADUATE SCHOOL
December 2004

Author : Cheak, Seck Fai

Approved by : Gamani Karunasiri
Thesis Advisor

Richard Christopher Olsen
Co-Advisor

James Luscombe
Chairman, Department of Physics

THIS PAGE IS INTENTIONALLY LEFT BLANK.

ABSTRACT

Traditionally, digital imaging systems rely on the use of dedicated photodetectors to capture specific wavelengths in the visible spectrum. These photodetectors, which are commonly made of silicon, are arranged as arrays to capture the red, green and blue wavelengths. The signal captured by the individual photodetectors must then be interpolated and integrated to obtain the closest color match and the finest possible resolution with reference to the actual object. The use of spatially separated detectors to sense primary colors reduces the resolution by a factor of three compared to black and white imaging. The FOVEON detector technology greatly improves the color and resolution of the image through its vertically arranged, triple well photodetector. This is achieved by exploiting the variation of absorption coefficient of silicon with wavelength in the visible spectrum. Hence, in a silicon detector, the shorter wavelength (e.g. blue) would be mainly absorbed at a shallow depth. A longer wavelength (e.g. red) would penetrate the material deeper than the shorter wavelengths and be primarily absorbed at a greater depth. By producing a layered silicon detector, all three primary colour wavelengths of red, green and blue can be captured simultaneously. This thesis aims to study the FOVEON camera's ability to image light from the near Infrared (NIR) to the Ultra-Violet (UV) range of the electromagnetic spectrum. The imaged obtained using a set of bandpass filters show that the camera has response both in the UV as well as NIR regions.

THIS PAGE IS INTENTIONALLY LEFT BLANK.

TABLE OF CONTENTS

THIS PAGE IS INTENTIONALLY LEFT BLANK.

LIST OF TABLES

THIS PAGE IS INTENTIONALLY LEFT BLANK.

LIST OF FIGURES

SYMBOLS

$S_{ref}(\lambda)$	Current measurement by the reference detector (μA)
$R_{reft}(\lambda)$	Responsivity of the reference detector (A/W)
$P_{ref}(\lambda)$	Radiant power detected by the reference detector (mW)
$I(\lambda)$	Intensity of light detected by the reference detector (W/m^2)
$A_{ref}(\lambda)$	Area of the reference detector array (m^2)
$S_{\text{det}}(\lambda)$	Current measurement of the FOVEON detector (μA)
$R_{\text{det}}(\lambda)$	Responsivity of the FOVEON detector (A/W)
$P_{\text{det}}(\lambda)$	Radiant power detected by the FOVEON detector (mW)
$A_{\text{det}}(\lambda)$	Area of the reference FOVEON array (m^2)

THIS PAGE IS INTENTIONALLY LEFT BLANK.

ACKNOWLEDGEMENTS

The author would like to extend his appreciation for the support and guidance received during the course of the thesis research. First, the guidance and patience given by Professor Gamani Karunasiri and Professor Richard Olsen were invaluable. Their advice has not only provided the author with a better understanding and appreciation of the optoelectronics and digital imaging, it has broadened the author's appreciation for scientific research and the hard work and imagination it requires. Second, the author would like to thank Mr. Dave Gilblom from Alternative Vision Corporation for his advice and contribution to the research. His willingness to share his expertise on the FOVEON image sensor has greatly eased the author's learning curve on the subject. Third, the technical assistance and sharing from MAJ Yeo Hwee Tiong is greatly appreciated. It has reduced the possible countless hours of trial and error in learning how to operate the lab equipment. Finally, the author would like to thank his wife Joyce. She has helped him keep his focus on the research and her understanding, support and love has been his motivation through the long hours. On the whole, it has been a thoroughly enriching and worthwhile experience.

THIS PAGE IS INTENTIONALLY LEFT BLANK.

I. INTRODUCTION

Imaging systems capable of discriminating spectral bands from the ultra-violet (UV) to the IR are increasingly important in the military. A comparison of the reflectance in the red and near infrared (NIR) wavelengths allows vegetation health to be determined. This principle also allows camouflage to be distinguished from surrounding vegetation by the judicious consideration of the spectral reflectance at various wavelengths. Other uses are also emerging with the maturity of spectral technology. Presently, there is an important need for imaging systems to have good spectral fidelity but yet be inexpensive. Current standard imaging systems (color focal planes) are poorly suited for such applications. A triple-well photodetector focal plane array, marketed as the FOVEON image sensor, was introduced into commercial availability in 2000. Compared to conventional photodetector arrays that only detect a relatively broad band of wavelengths, the FOVEON image sensor is able to discriminate three different visible wavelengths of light (blue, green and red) on each individual pixel. The purpose of this thesis was to study the ability of the triple-well FOVEON camera to image light from the NIR to the UV wavelengths from 200 nm to 1100 nm. This was achieved by measuring the signal outputs at each of the three detectors (red, green and blue) in the FOVEON camera for the range of wavelengths mentioned above.

A. TECHNICAL BACKGROUND

The semiconductor photodetectors have become a critical component in many modern sensing and imaging devices, such as compact disc players, digital cameras and video cameras. Photodetectors may be broadly separated into photoconductors and photodiodes. Photoconductors work on the principle of exciting electrons from the valence band to the conduction band when photon energy is greater than the bandgap of the material. Under an external bias, these electrons produce a current in the material which is converted into a voltage signal by measurement devices or into a binary code by microchips within the image sensor. The binary codes represent image information such as color and brightness.

Photodiodes consist of a p-n junction where the built-in electric field can generate either a photocurrent or a voltage depending on the mode pf operation as illustrated in Figure 1. A reverse bias is usually applied to the photodiode to increase the depletion layer width that results in a higher responsivity. The disadvantage of these single-layered conventional photodetectors is that a specific band of wavelengths may be detected without the spectral information, depending on the bandgap of the semiconductor, E_g. Therefore, in the area of color imaging, different detectors are required to capture the three primary colors of the visible spectrum. This is achieved by placing micro-filters in front of the photodetectors to ensure selective wavelengths are captured. These detectors are often arranged in the form of a Bayer array pattern [1]. Each detector acts as an image pixel and represents the intensity of one of the primary colors that make up the input image. In order to accurately reproduce the actual image, various signal processing techniques are required to integrate as well as interpolate the pixilated signals. The techniques aim to reproduce the correct color match and image brightness, as well as to provide as high a resolution as possible. One of the disadvantages of this approach is the loss of spatial resolution since three spatially separated detectors needed for capturing the color information. Many different materials may be used to produce photodetectors, including Silicon (Si), Gallium Arsenide (GaAs) and Indium Antimonite (InSb); however, Si is primarily used for visible light detection due the possibility of monolithic integration of signal processing electronics. [2]

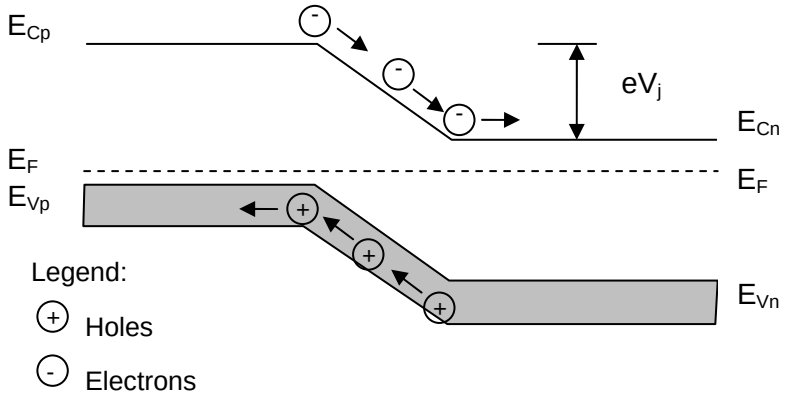

Figure 1. Band Diagram of a PN Junction Photodetector adapted from [2].

To circumvent the drawbacks posed by single-layered detectors, FOVEON developed a triple-well photodetector which can sense the three primary colors in the same pixel. This is achieved by making use of the intrinsic characteristic of silicon to absorb different wavelengths of light according to its thickness. The absorption depth of Si with wavelength is shown in Figure 2. Shorter wavelengths (blue) would be absorbed by a thin layer of silicon near the surface whilst longer wavelengths (green and red) would pass through the surface layer of silicon and be absorbed only in the underlying layers. Stacking three p-n photodetectors at different depths, as shown in Figure 3, allow the collection of signals from different wavelengths in the same pixel. Each layer of silicon is doped with different levels of n and p type dopants to form the p-n junctions. With the application of a small reverse bias voltage, each layer acts as one end of a PN junction to the next. This produces higher sensitivity and allows easy signal readout. According to the US patent report for the FOVEON image sensor [3], this idea was not totally novel since there have been previous attempts to use layered or stacked photodetectors to perform this function. These designs were, however, extremely expensive as a commercial product and complicated to manufacture and assemble. It was largely due to the recent advances in Complimentary Metal-Oxide Semiconductor (CMOS) fabrication techniques that the FOVEON detector technology could be produced with commercial viability.

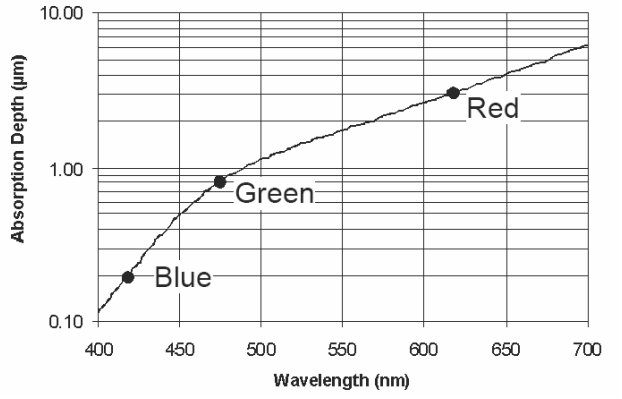

Figure 2. Absorption Depth of Silicon with Wavelength. The photodetectors used in FOVEON camera are located at the three depths of 0.2 μm, 0.8 μm and 3 μm [4].

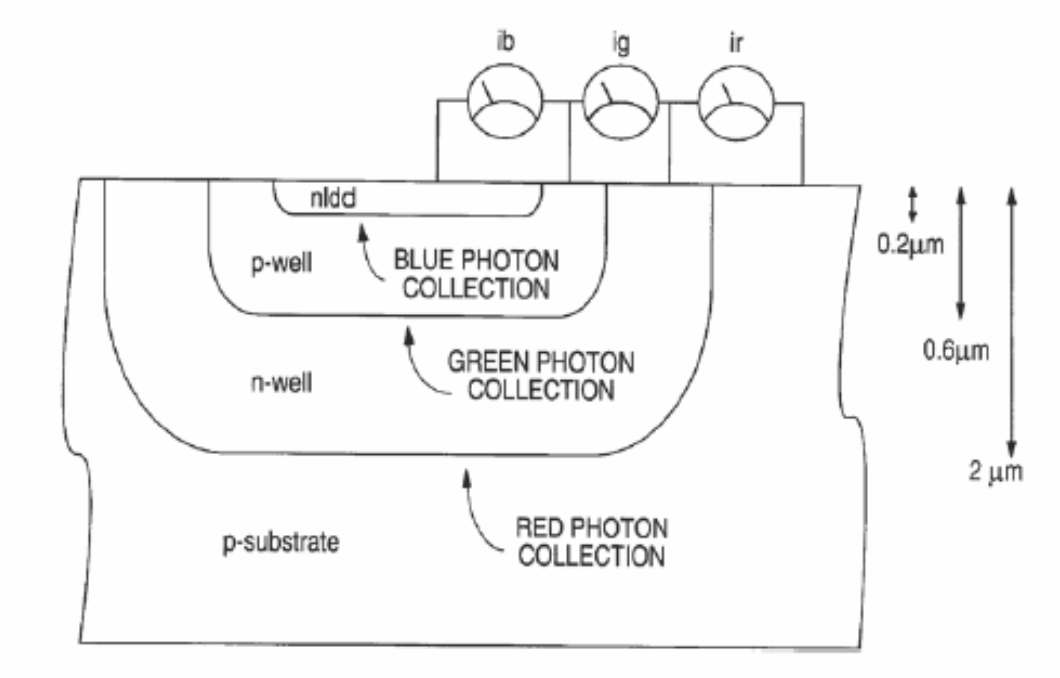

Figure 3. Schematic showing the three p-n junctions in a FOVEON pixel [3].

According to FOVEON Inc. press releases, its patented photodetector is able to achieve color resolutions three times higher than conventional photodetectors arranged in the Bayer pattern [4]. Since every pixel of the image is detected by a single photodetector, the FOVEON detector is able to capture three wavelengths coming from the image, rather than a single wavelength, producing brighter images and better color representation of the image scene. Conventional photodetector technology would not only lose image brightness but require complex image post-processing techniques such as interpolation to obtain a close color match. According to reviews and articles published on the World Wide Web, the quality of digital images captured by the FOVEON photodetector may even be comparable to the photo-emulsion films used in traditional color photography [5]. The CMOS design of the image sensor also allows processing to be performed at the pixel, reducing the size required of the image sensor. It also allows pixels to be grouped together in high frame rate, low resolution applications [6]. At the time of writing, the FOVEON detector technology has been employed in a number of commercial digital

cameras with positive feedback. Judging from the lack of published literature except one [7], it is assumed that not many attempts have been made to expand the detection spectrum of the FOVEON detector to include both the near-UV and near-IR ends of the visible spectrum.

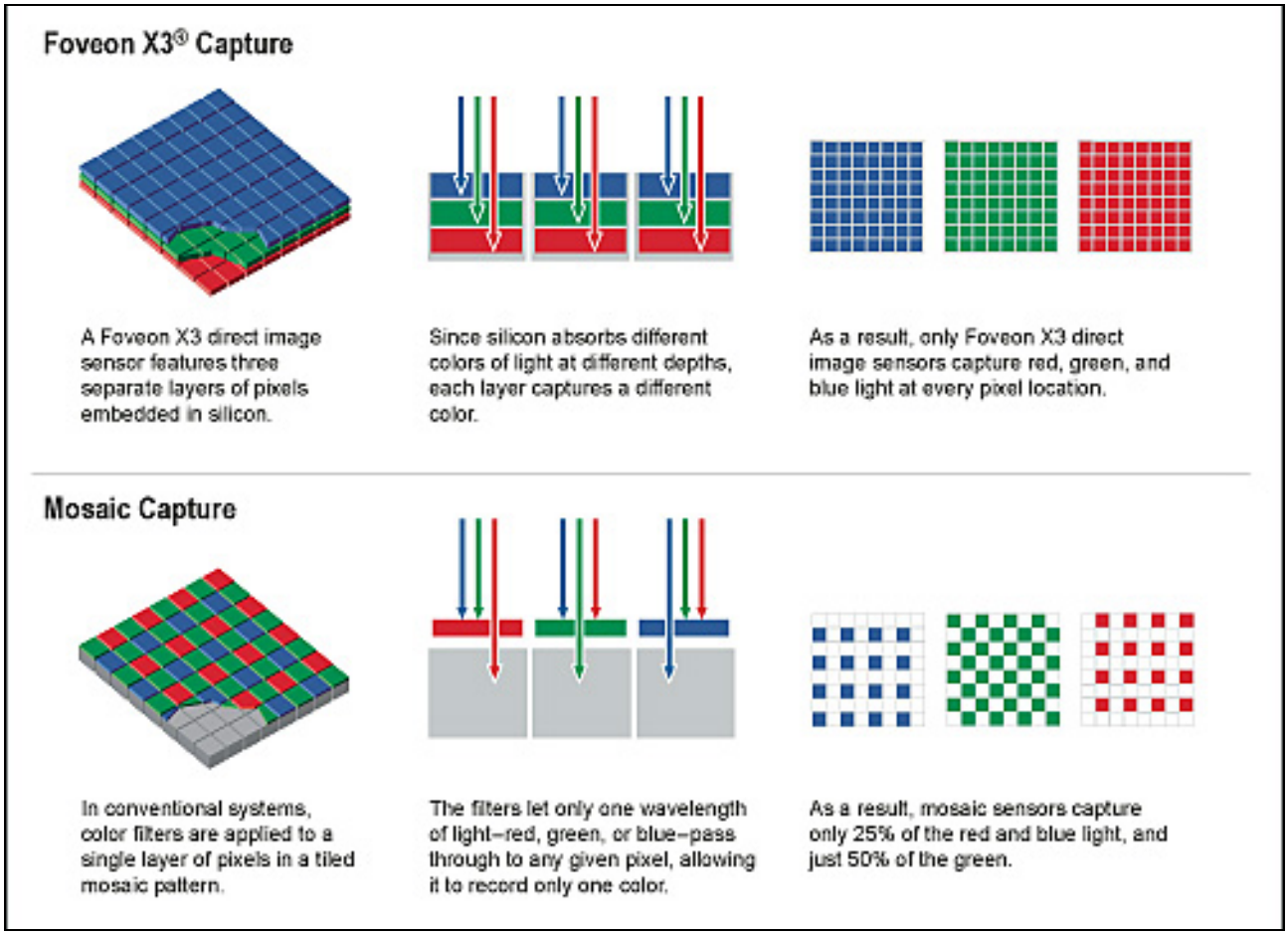

Figure 4. Comparison of FOVEON Detector Technology (above) with Conventional Silicon Photodetector Arrays arranged in the Bayer pattern (below) [1].

There are many potential applications for the FOVEON image sensor. The military employs numerous imaging systems in the various services for observation, surveillance, targeting, navigation and tracking purposes. The accuracy and validity of the analyses derived from these systems are crucial to the success of military operations and the reduction of mistakes and unnecessary loss of life. Hence, by employing the FOVEON detector technology in its image analysis and surveillance

activities, the military stands to benefit from its higher resolution and more accurate imaging capabilities. A high level of detail in images allows for better intelligence collection and precision strike planning. The technology employed for intruder detection and other target acquisition systems that rely on high image detail may also be further improved with the FOVEON photodetector. Further benefit may be derived by the extended detection spectrum to include UV and near IR wavelengths. Applications that will stand to gain from this research include night vision sighting equipment and target tracking systems, both applications employing the advantages of operating in the near IR wavelengths. Near-UV imaging applications include anti-camouflage applications as well as applications to reduce image blooming caused by high intensity background lighting.

B. STRUCTURE OF THESIS

This report documents the background theory and experimental procedures employed to achieve the goal of the thesis. It is divided into five chapters. The first chapter introduces the theoretical background behind photodetectors and outlines the structure of the research. The second chapter explains the characterization procedures of the FOVEON detector in detail. The third chapter discusses the images captured in the near-IR and near-UV wavelengths as well as the theory behind the perception of color and color image processing. The fourth chapter discusses the findings from the thesis and various proposals for further study. The final chapter concludes. The various appendices present detailed findings of this thesis as well as detailed equipment specifications used in the course of thesis research.

In the course of this report, the term “FOVEON detector” or “FOVEON image sensor” will be used to mean the entire FOVEON detector array installed in the HanVision camera, unless otherwise stated. The term “camera” or “HanVision camera” will be used to mean the HanVision HVDUO-5M camera purchased for the thesis research. The term “monochromator” refers to the photodetector characterization system set up in the Naval Postgraduate School Sensor Research

Lab (SRL). The term “invisible” is a generic reference to the near-UV and near-IR wavelength regions that are the focus of study in this thesis.

C. SYSTEM OVERVIEW

1. General

For the purpose of this thesis, the HanVision HVDUO-5M camera, fitted with a FOVEON X3 image sensor, was used. It has 8-bit digital output for each of the colors and is capable of recording images in the range of wavelengths of interest. It is packaged with a number of software applications to control the various modes and functions of the camera, as well as to perform image analysis. Additional information on the camera may be obtained from the HanVision company website [8]. The thesis research involved the characterization of the FOVEON detector array in the camera and subsequently, capturing images in the near-UV and near-IR wavelengths. In the characterization phase, the responsivity of the FOVEON detector array as a function of wavelength was measured using a monochromator and a calibrated photodiode. Next, images were captured using the camera and suitable optical filters before undertaking further post-processing development. The equipment and software products required for this purpose are summarized in Table 1.

S/No.	Equipment	Remarks
1.	Oriel Monochromator System.	The photodetector characterization system set-up in the NPS SRL by LCDR Herdlick, USN [9].
2.	HanVision HVDUO-5M Imaging Camera.	Research grade imaging camera with FOVEON detector technology.
3.	Matrox Meteor II/ Camera Link Framegrabber card.	Image capture device to interface HanVision Camera with analysis PC.
4.	Calibrated UDT Sensors UV-035D Planar Diffused UV Enhanced Photodiode (S/No. 7309) 0.	Calibration of the monochromator and FOVEON camera.
5.	Matrox MIL-Lite 7.5	Image capture software for the HanVision Camera and driver utility for the Framegrabber card.
6.	National Instruments Labview 6.0.	Driving software for the monochromator.
7.	NEGUS	HanVision Image Analysis Software.
8.	HCCT	HanVision Image Capture Software.

Table 1. List of Equipment used in the camera characterization and imaging.

Further discussion on the experimental set-up is presented in Chapter II of this report while additional technical information and specifications of the research equipment may be found in the Appendices.

2. Characterization of the FOVEON Image Sensor

Characterization of the FOVEON detector array was done in a number of steps. First, the intensity output of the monochromator at various wavelengths was calibrated. This was achieved by using a calibrated UV enhanced photodiode (see Appendix I for calibration data), across a spectrum of light from 200 nm to 1200 nm in wavelength.

If the responsivity of the calibrated detector is $R_{ref}(\lambda)$ and power incident on the detector is $P_{ref}(\lambda)$ then the measured current signal $S_{ref}(\lambda)$ can be calculated as follows :

$$S_{ref}(\lambda) = R_{ref}(\lambda) \times P_{ref}(\lambda) \qquad \text{---------- (1)}$$

Thus, the power incident on the photodetector is given by

$$P_{ref}(\lambda) = \frac{S_{ref}(\lambda)}{R_{ref}(\lambda)} \qquad \text{---------- (2)}$$

The intensity of the light incident on the photodiode can be calculated using the calibrated detector area ($I(\lambda)$) as:

$$I(\lambda) = \frac{P_{ref}(\lambda)}{A_{ref}(\lambda)}$$

$$= \frac{S_{ref}(\lambda)}{A_{ref}(\lambda) \times R_{ref}(\lambda)} \qquad \text{---------- (3)}$$

Next, the HanVision Camera was coupled to a computer using the Matrox Meteor II/Camera Link Framegrabber and the signal output from the different detector layers of the FOVEON camera was recorded. The signal response of the FOVEON detector was retrieved and analysed using the two software applications provided by HanVision. The HCCT software, provided by the camera manufacturer, was used for sending image capture commands to the camera, as well as applying the various exposure and color compensation settings. Images captured were transferred to the NEGUS software to extract the red, green and blue signal responses from the image sensor. The raw voltage measurements from the individual pixel photodetectors were converted into a digital binary code by the image processing electronics within the camera. These 8-bit digital data, represented the 0 to 255 monochrome values for each color. These values were then normalized to obtain the responsivity curves of the image sensor. The process of measurement was similar to the calibration of the monochromator power using the

calibrated photodetector. Multiple measurements were performed to study the effects of the camera's exposure time and other settings on the responsivity measurements.

The responsivities of the three detectors at each pixel $R_{det}(\lambda)$ can be obtained the measured signal ($S_{det}(\lambda)$) and area of the detector ($A_{det}(\lambda)$) as follows :

$$S_{\det}(\lambda) = I(\lambda) \times A_{\det}(\lambda) \times R_{\det}(\lambda) \quad \text{---------- (4)}$$

$$R_{\det}(\lambda) = \frac{S_{\det}(\lambda)}{\frac{P_{ref}(\lambda)}{A_{ref}(\lambda)} A_{\det}(\lambda)}$$

$$= \frac{S_{\det}(\lambda)}{\frac{S_{ref}(\lambda)}{R_{ref}(\lambda)} \left(\frac{A_{\det}(\lambda)}{A_{ref}(\lambda)} \right)} \quad \text{---------- (5)}$$

In the course of the research, it was found that there were certain limitations in the dynamic range of the camera especially when the signal strength is weak for UV and NIR wavelengths. Hence, different camera settings and focusing optics were used to enhance the signal strength. Care was taken to ensure that these parameters, such as lamp current and focusing of the light source for the photodiode and camera measurements were compatible for different experiment scenarios. These limitations will be discussed in detail in the following chapters of this report.

3. Near-UV and Near-IR Imaging with the FOVEON Camera

Although, the FOVEON image sensor is designed primarily to capture visible light (450 – 700 nm), it is also able to detect near-UV and near-IR wavelengths as well. According to studies performed by Gilblom and Yoo [7], the FOVEON detector captures near-UV photons in the top layer of the photodetector, in the region designed to capture blue light. It also states that near-IR wavelengths would pass through all three layers, due to its longer wavelength, and produced detection signals primarily in the bottom layer. This particular characteristic of the image

sensor was essential in the image capture of near-UV and near-IR wavelengths. Image capture and analysis are further elaborated in Chapter III of this report.

THIS PAGE IS INTENTIONALLY LEFT BLANK.

II. CHARACTERIZATION OF THE FOVEON DETECTOR ARRAY

A. GENERAL

Responsivity describes the current or voltage produced by the photodiode when light of a given power impinges on it. Responsivity varies for different wavelengths and normally peaks around the bandgap energy of a photodiode [2]. The first step in the thesis was to determine the responsivity of the FOVEON detector array as a function of wavelength. The responsivities of the three photodiodes associated with each pixel showed the sensitivity of the detector to various wavelengths of light. This was achieved by first calibrating the monochromator using a factory calibrated UV enhanced photodiode. The signal responses of the three photodetectors were measured next. From Equation 5, their responsivities for various wavelengths were calculated. Due to the low power output of the monochromator at near-UV and violet wavelengths, the blue gain of the camera was increased, whilst suppressing the red and green response of the detector. This provided higher signal output at those wavelengths. This chapter presents the experimental set-up and measurement procedures adopted.

B. EQUIPMENT AND SOFTWARE SET-UP

1. Hardware Set-Up

The hardware set-up for the spectral measurement was straightforward and primarily involved the Oriel Monochromator system assembled by LCDR Herdlick [9], as well as the installation of the Matrox Meteor II Framegrabber card to control the HanVision camera. Without any major adjustments to the layout of the system, the photodiode and the camera were mounted in the same location on the optical table for the monochromator light intensity measurements and the camera characterization, respectively. This is shown in Figure 5 and Figure 6. While slight adjustments were made to focus the light onto the detector arrays, their position remained relatively close and may be assumed to be the same. The technical and operating details of the Oriel monochromator have been well documented in

Herdlick's thesis [9] and will not be covered in this report. The photodiode selected to calibrate the light intensity output of the monochromator was the UDT UV enhanced UV-035D Photodiode (see Figure 8), chosen due to its sensitivity in the UV range. It was factory calibrated from 200 nm to 1100 nm wavelength range (See Appendix I for more information). The calibrated photodiode was connected to one of the lock-in amplifiers which read the photocurrent generated by the photodiode. From the measurements, it was found that the monochromator output had extremely low intensities in the near-UV and violet-blue region (from 200 nm to 400 nm) of the spectrum. It was necessary to focus the light from the monochromator to increase the intensity of light incident on the calibrated photodiode and the camera. Note that the focused light is incident only the middle section of the FOVEON array.

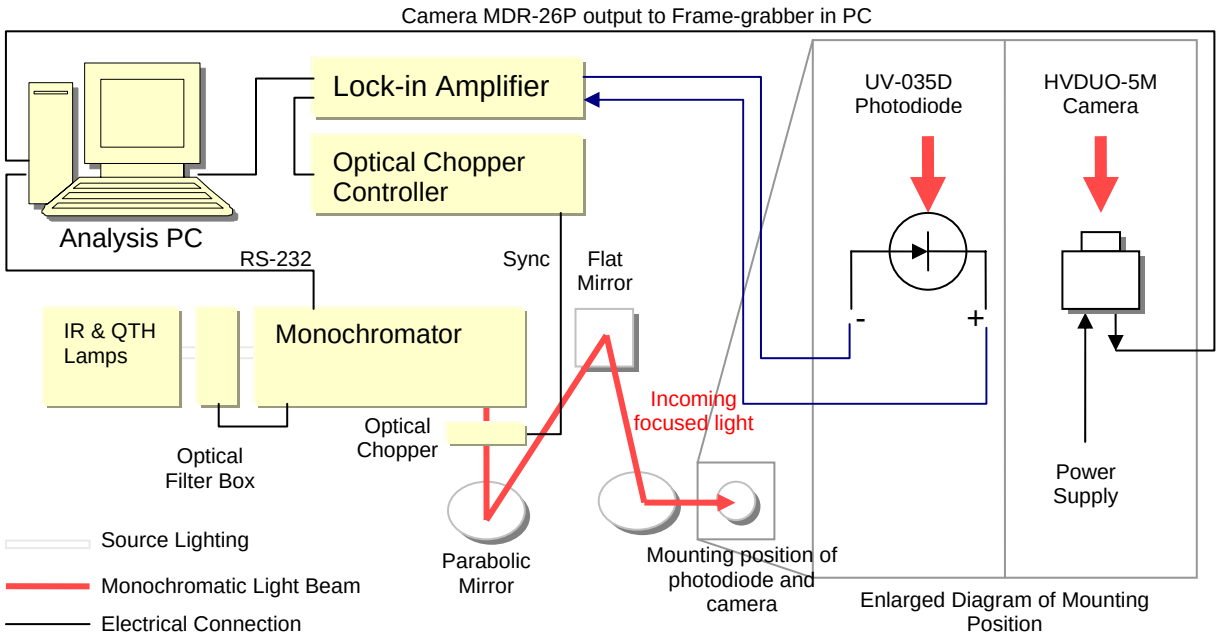

Figure 5. Block Diagram of Hardware Set-up

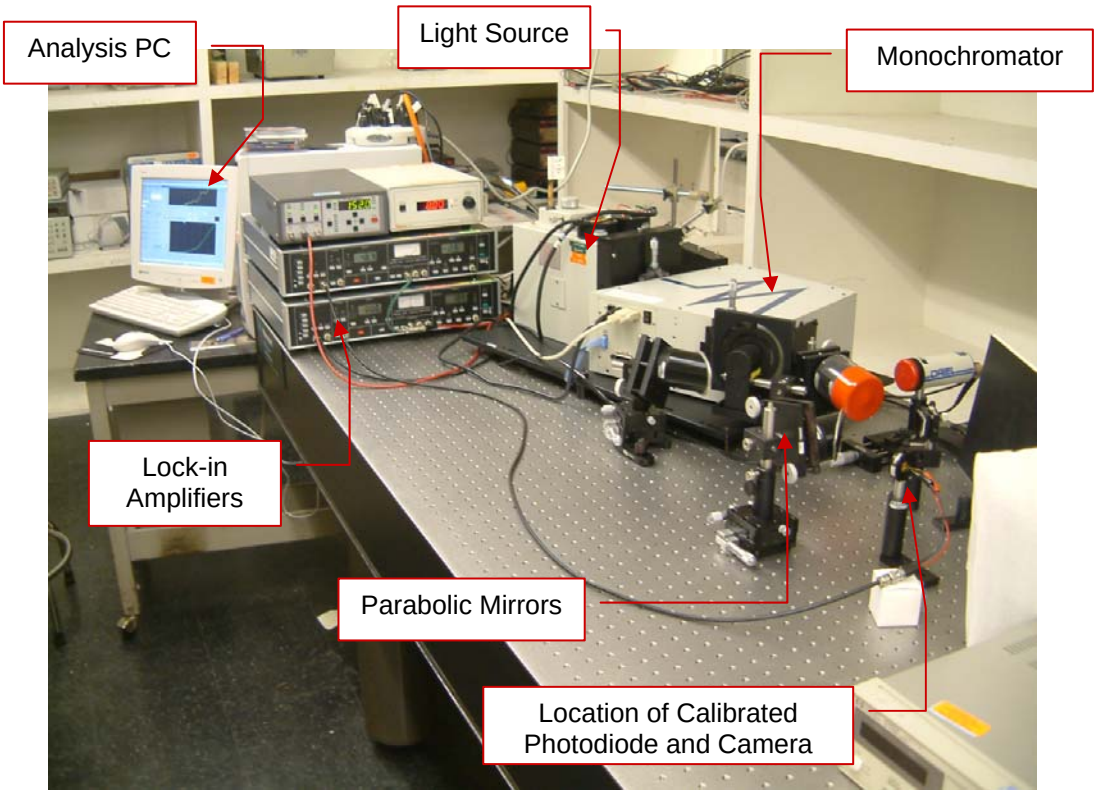

Figure 6. The Oriel Monochromator System used in the Measurement.

There was an initial attempt to apply a reverse bias voltage to the calibrated photodetector but it was found that the output signal was beyond the lock-in amplifier range. The photodiode was still able to detect the light input extremely well without the bias. This was verified by comparing the resulting responsivity curve with information contained in its product brochure [10]. As such, the calibration proceeded without any external bias in the photodiode. Due to the high sensitivity of the photodiode and the maximum detection limits of the lock-in amplifier, the output slit width of the monochromator was adjusted to 0.5 mm. The current in the monochromator light source was set to either 7 A out of maximum 8.33 A. The lower current setting was used primarily for the measurements beyond 400 nm in order to prevent saturation of the signal on the camera or the photodiode. The higher lamp current setting provided more power when measuring the shorter wavelengths (less than 400 nm) of light. Due to the limitations in the measurement

equipment, care was taken to prevent signal overloading yet attempting to maintain sufficient signal strength for the measurement. As such, the calibration of the monochromator light intensity was done with multiple settings in order to select the optimal result set for analysis. Another measure adopted to prevent overloading was the focusing of the monochromatic light on the detectors. Measurements were taken with the tightly focused light on the detector as well as spread over the detector area as illustrated in Figure 7. Optical filters were used to filter the monochromator light source in order to minimize the second order effects from the gratings. In addition, the effects of the room lighting were also studied by performing the calibration both with the room lighting on and another time with it switched off. In both cases, the results show negligible differences. Data with the same experiment parameters were used in the calculation of the responsivity values. A summary of the experiment parameters for the calibration of the monochromator light intensity using the photodiode is shown in Table 2.

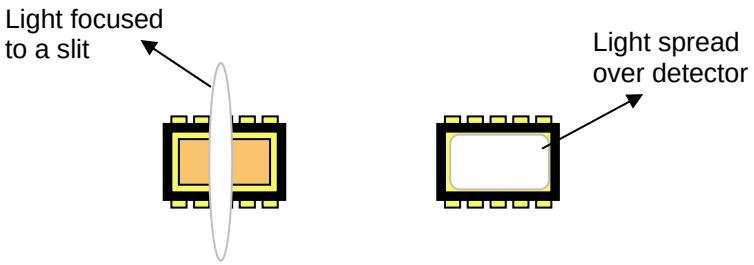

Figure 7. Schematic diagram of monochromatic light beam focused on the detector (left) and spread over detector (right).

Parameter	Value	Parameter	Value
Optical Chopper Frequency	152 Hz	Photodiode Bias Voltage	Nil
Photodiode Peak Wavelength	970 nm	Photodiode Detector Array Area	5.8 x 5.8 mm^2
Monochromator Illuminator Current Output	7 A	Monochromator Output Slit Width	0.5 mm
Minimum Monochromator Output Wavelength	200 nm	Maximum Monochromator Output Wavelength	1100 nm
Monochromator Output Wavelength Interval	10 nm	Time Interval between signal recording	5 s
Measurement Range 1 (no filter used)	200 to 500 nm	Scale on Lock-in Amplifier (Current setting 10^6 V/A)	30 mV (light spread), 300 mV (light focused)
Measurement Range 2 (420 nm filter used, light spread over detector and light focused)	400 to 700 nm	Scale on Lock-in Amplifier (Current setting 10^6 V/A)	3 V
Measurement Range 3 (620 nm filter used, light spread over detector and light focused)	600 to 1200 nm	Scale on Lock-in Amplifier (Current setting 10^6 V/A)	3 V

Table 2. Experimental Settings used for Calibrating Monochromator Light Output.

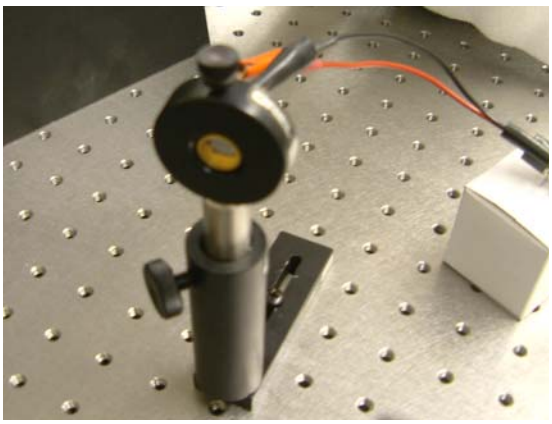

Figure 8. The UDT UV-350D Photodiode mounted on the optical bench.

The responsivity of the FOVEON camera was measured next. Although the HVDUO-5M camera only had 1.51 million individual photodetector elements, it had a total color resolution of 4.53 megapixels due to its triple layered structure. It has a 24-bit digital output (8-bits for each color) and is able to capture both still and video images. The camera had flexible exposure settings and other image control features that were useful for the purpose of the research. For image capturing, the camera was connected to a PC. The lens of the camera is transparent to near UV wavelengths.

Figure 9. The HanVision HVDUO-5M Camera (left) [8] and the internal FOVEON X3 Image Sensor (right) [4].

No major changes were made to the hardware set-up from the first stage except that the camera was placed in the position of the photodiode and connected to the PC by means of a RS-422 cable via the framegrabber. The same routines were conducted with the monochromator scanning wavelengths from 200 nm to 1100 nm. The digital signal readouts were recorded from the line profile tool in the NEGUS application. Since the optical chopper was not employed, the calibration of the camera was performed in a darkened environment to minimize the signal due to room lighting. Although similar procedures were followed, the camera measurements were performed in multiple stages to adjust for the effects of exposure time and other camera settings during the responsivity measurement. Measurements were also taken with the built-in camera filter (400 to 660 nm) on and

subsequently removing it. The Table 3 summarizes the experimental settings for measuring the camera responsivity. Further details about the camera software settings are discussed in the following section.

S/No.	Camera Experiment Setting					
	Lamp Current (A)	**Wavelength Range (nm)**	**Monochromator Filter (nm)**	**Gray Mean Value**	**Exposure Timing (ms)**	**Focusing of Monochromatic Light**
1.	8.33	200-500	None	None	12.5	Focused Slit
2.	8.33	200-500	None	-10, -10, 20	25	Focused Slit
3.	8.33	200-500	None	-10, -10, 20	12.5	Focused Slit
4.	7.0	400-700	420	None	12.5	Spread over detector
5.	7.0	600-1200	620	None	12.5	Spread

Table 3. Experiment parameters for measuring the HVDUO-5M responsivity.

2. Software Set-Up

There were two main programs that were used to run the experiment. The first was the existing LabView program compiled by Herdlick [9] to operate the entire monochromator system. It primarily controlled the monochromator and recorded of the voltage readouts from the lock-in amplifiers.

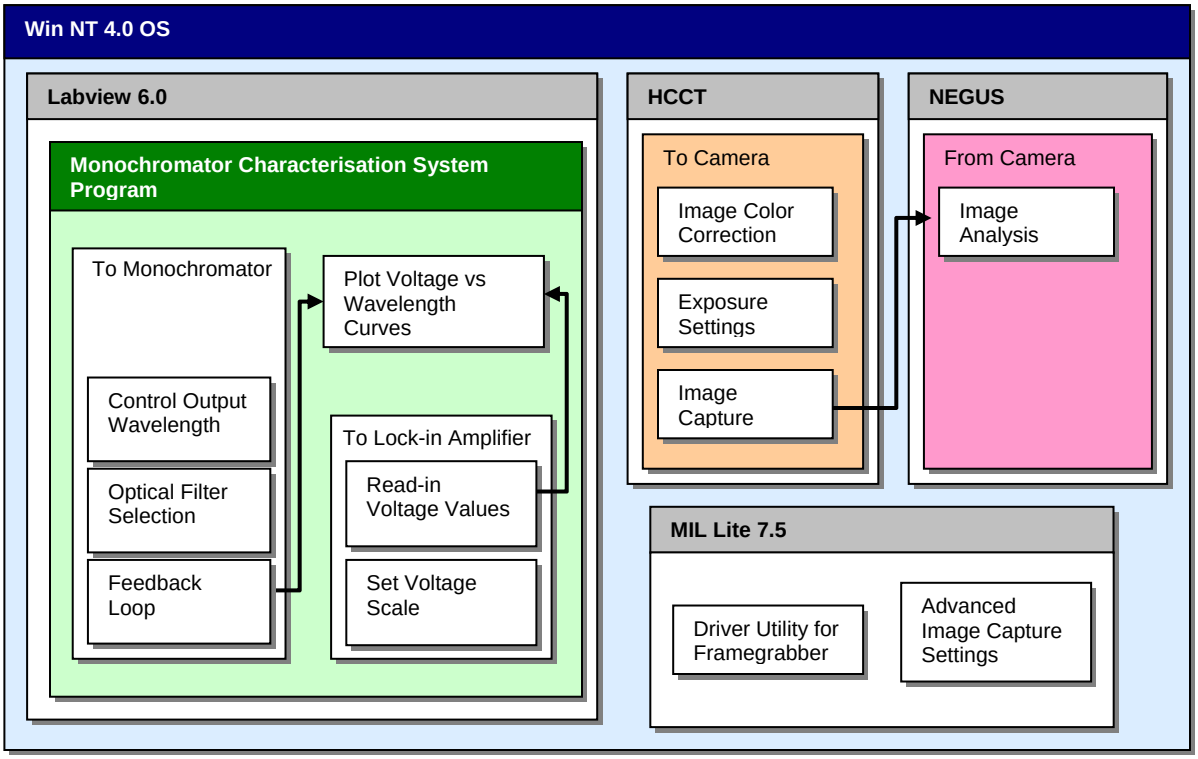

Figure 10. Block Diagram of Software Linkages and some Key Functions.

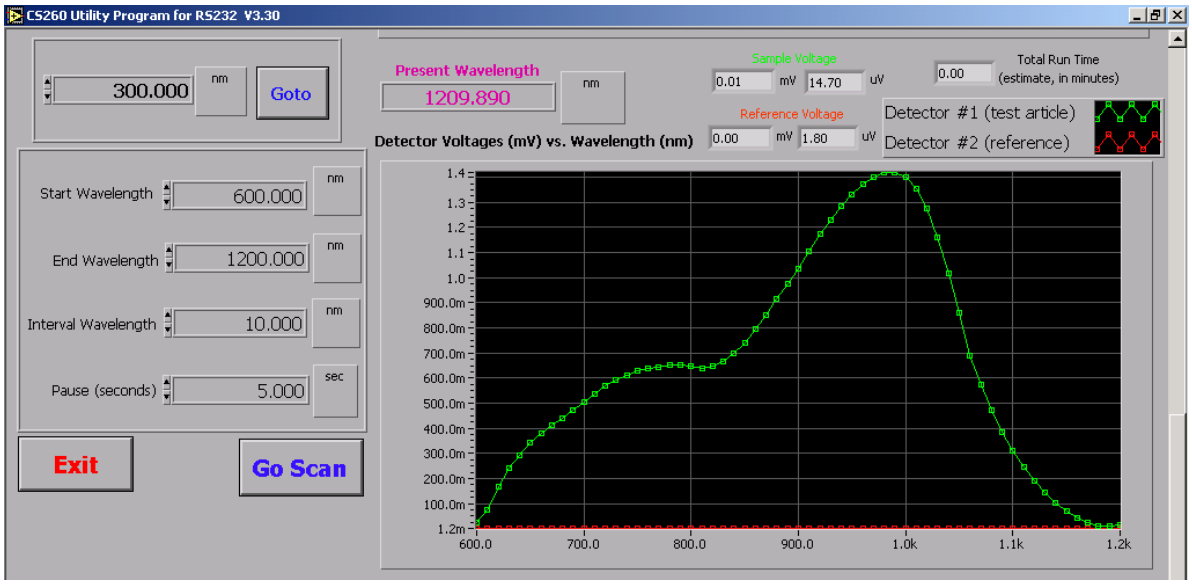

Figure 11. Screenshot of LabView Monochromator Control Program.

The other programs running simultaneously with LabView were the HCCT and NEGUS programs. The HCCT program provided simple software interfaces to

adjust the color compensation, exposure time, shutter and other settings for the HVDUO-5M camera [11]. Built into the camera was an image processing chip that translated signals generated by the three photodetector layers into sRGB color data for subsequent display. Depending on the color compensation settings, this translation may produce images with varying hue adjustments. Therefore, in order to obtain the most accurate color captured by the camera, it was necessary to disable the camera's color adjustment function by setting the color settings to "unit". To improve the signal measured in the shorter wavelengths (200 nm to 400 nm), the exposure time for the camera was increased and the Gray Mean Value was adjusted. The Gray Mean Value setting allows for the manual compensation of the individual red, green and blue signal outputs from the camera. This function was used to improve the detector response in the blue layer when capturing near-UV and violet light. In order for the image sensor to capture equal amounts of light at every pixel line, the shutter setting was set to rolling shutter.

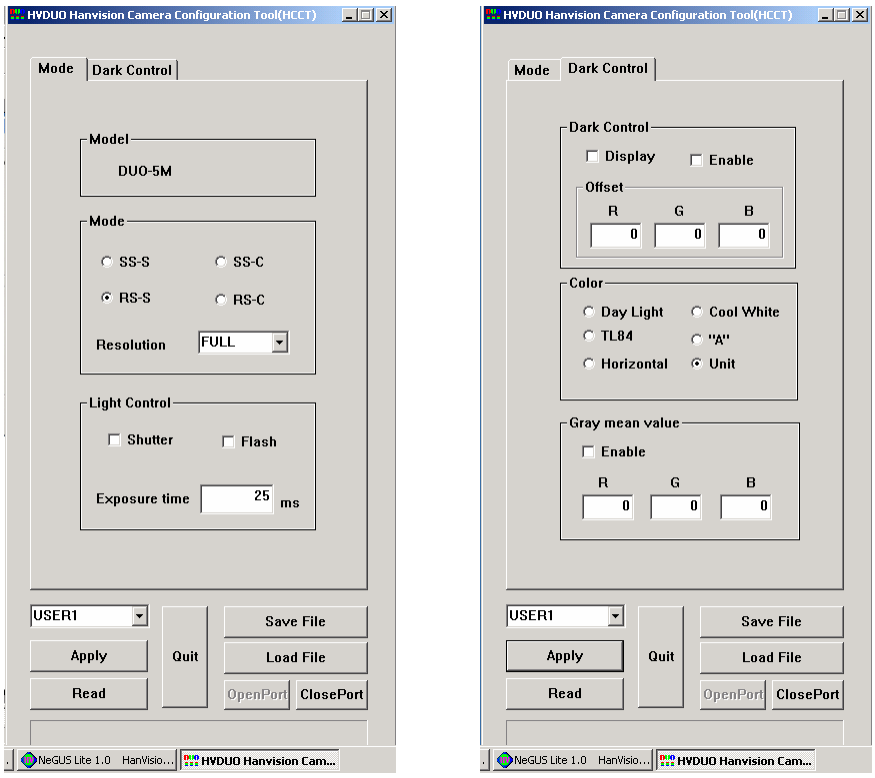

Figure 12. Screenshots of the HCCT software showing the interfaces for adjusting various image capture settings for the HVDUO-5M camera.

As shown in Figure 12, the HCCT software was used for controlling the camera settings. The HCCT software must be operated with the NEGUS software to receive and display the captured image. The NEGUS software has a number of simple interfaces with which to perform image analysis. The two main functions that were commonly used were the line profile and pixel histogram functions. As shown in Figure 13, the line profile function displayed the red, green and blue signal levels of the captured image, at a selected pixel line. Each color was represented by an 8-bit binary code to represent the 256 monochrome shades of that color. A combination of these three colors provided the 24-bit digital output and represented the color in an individual pixel. The line profile gave a quick indication of the color combination in the image as well as to whether there were too much dark colors or over-saturation in the image due to the camera's color compensation settings. Different experimental settings, such as increased lamp power and Gray Mean Value adjustments were made for images with extremely low signal output (especially in the shorter wavelength range mentioned). Selected regions in the image that were not oversaturated were used to obtain a balanced result. The pixel histogram tabulated the number of pixels for each shade of the three colors in the image. The mean value of the image for the individual color was also calculated. As shown in Figure 14, the 650 nm monochrome light is shown to consist of a combination of red, green and blue levels. Within each primary color is a distribution of the monochrome shades as well as the mean. When set to the "unit" color coefficient setting (on the HCCT program), this mean level was taken to be the nominal signal response for that primary color.

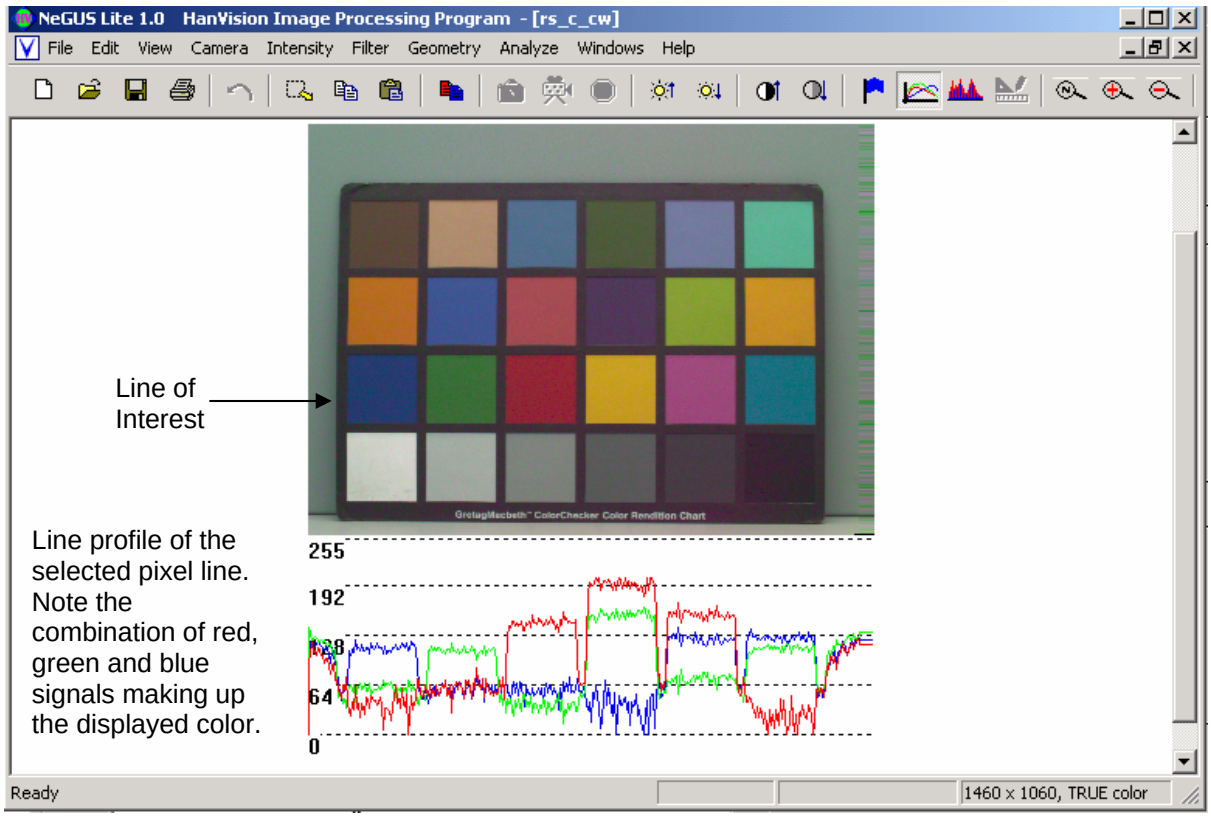

Figure 13. Screenshot of the NEGUS software showing the line profile function.

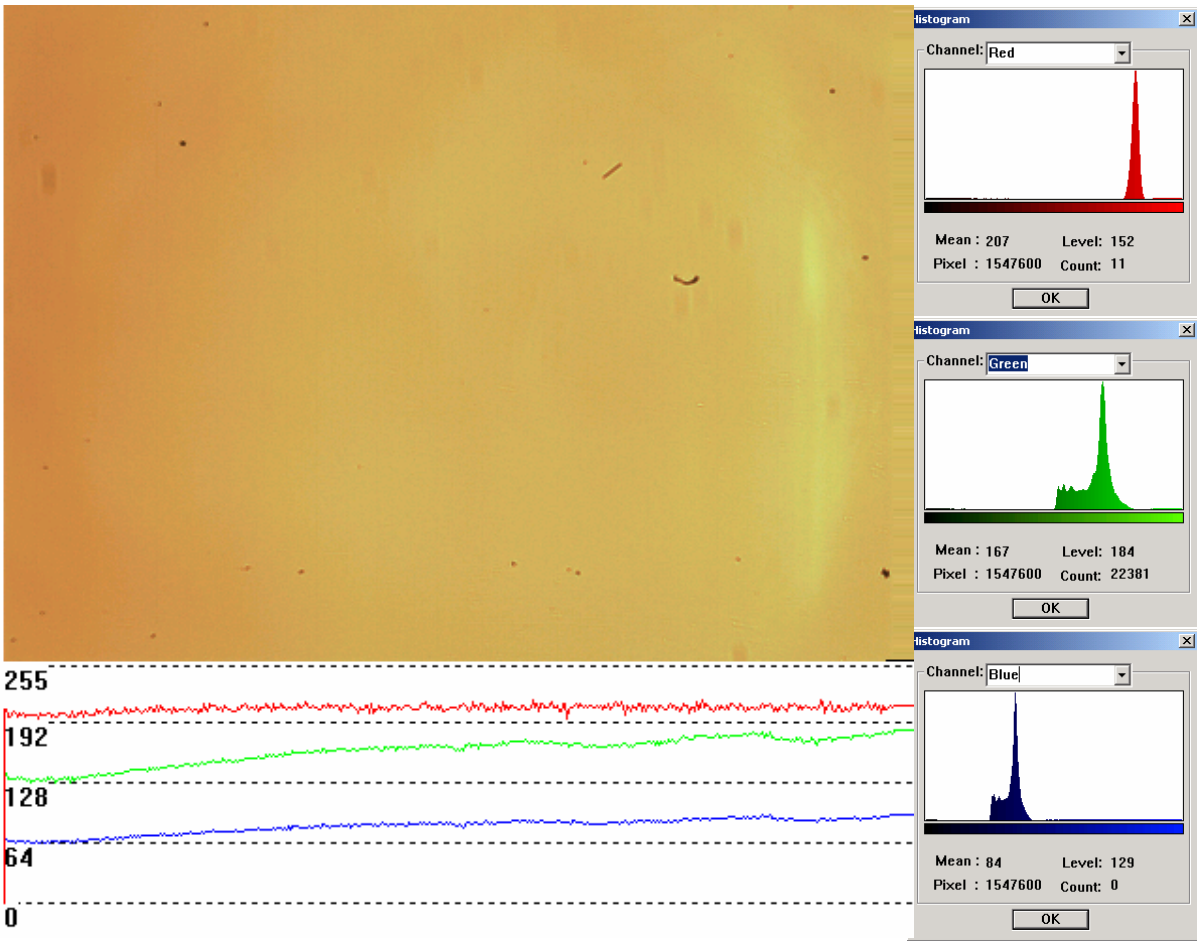

Figure 14. Image of a monochrome light at 650 nm wavelength showing the contribution from the red, green and blue signals.

3. Results

From the approach described in the previous chapter, the intensity of the monochromator was found to be as shown in Figure 15. The curves from different wavelength regions generally show continuity and overlap. As mentioned, the calibration measurement had to be done in stages with suitable optical filters applied to remove the contribution from second order effects. The results from each stage are represented by each of the curves. The sharp drop-off at 1100 nm was due to the long wavelength cutoff of the photodiode due to bandgap of silicon (1.12 eV at 300 K). It can be seen that intensity of the output of the monochromator varies with wavelength. It has peak intensity at approximately 1000 nm for a lamp current of 7 A. It is particularly weak in the near-UV and violet-blue regions of 200 nm to 400 nm.

This characteristic posed some challenges for the responsivity measurements for the camera. Due to the low light intensity at this region, the exposure time for the camera had to be set at 25 ms and Gray Mean Value adjustments made to the camera to capture more light. This caused over-saturation of the image sensor for the green and red signals beyond 400 nm. The Gray Mean Value function available in the HCCT software was used to reduce the red and green signals and boost the blue response. Multiple measurements were taken with different camera settings, as summarized in Table 3, to plot the camera response curve.

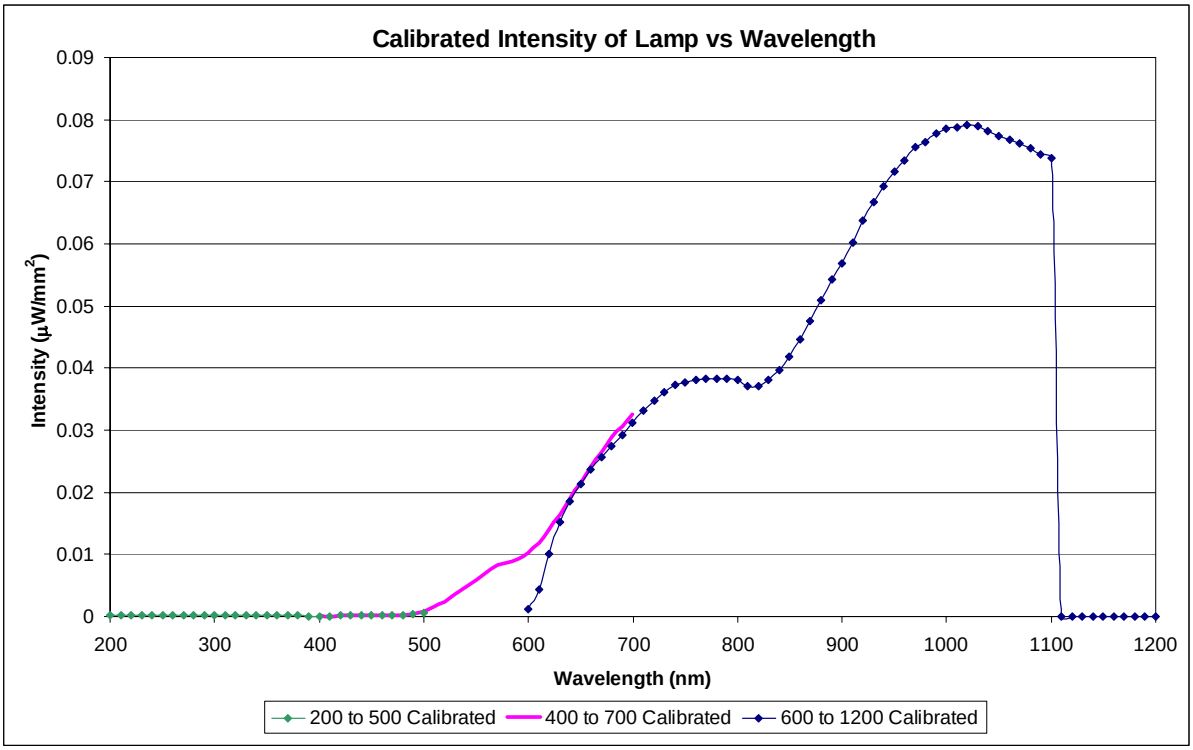

Figure 15. Calibrated Intensity of the Monochromator output vs Wavelength.

As mentioned, the measurements were taken with the monochromatic light spread over the calibrated detector, and a second setting with light focused on the detector. Similar settings were also used during the characterization of the camera. As the near-IR photons are captured in the red layer, the resultant image is artificially colored by the camera image processor to display it in a reddish color. For

the second case with focused light, the entire area of the image was analysed as the signals were not oversaturated even with the Gray Mean Value adjustment.

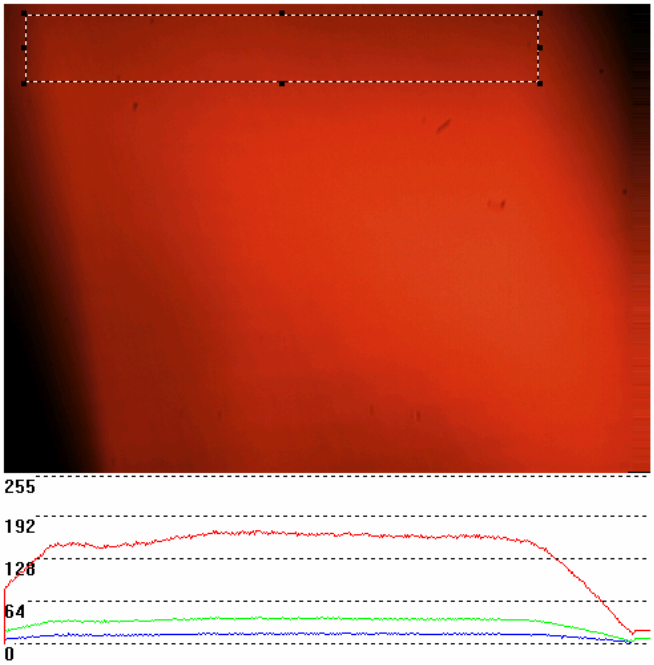

Figure 16. Image of 1000 nm wavelength monochromatic light. Since most of the signal at this wavelength comes from the bottom sensor, the software assigns it red color.

Numerous measurements were taken with camera in various configurations. This was to study the effects each setting had on the results as well as to select the most suitable result for analysis. It was important that the captured images were not over-compensated by the camera's internal image processor, yet had a sufficient range of signal response. The most suitable experimental set-up was with the monochromator light source current set at 7 A for light spread over the detector and at 8.33 A for light focused. The camera exposure setting was at 25 ms and the monochromator slit widths at 0.5 mm. Figure 17 shows the estimated FOVEON responsivity in the visible region (with the camera filter in place). The response curves are similar to that generated by FOVEON [12]. The undulating profiles of the curves are due to the insufficient dynamic range of the camera. The 8-bit digital output for each color was not sufficient to provide the required signal resolution needed to plot smoother curves. The lock-in amplifiers had an analog measurement range from less than 3 mV to more than 3 V which is equivalent to a 10-bit digital

output. However, the HVDUO-5M camera could only produce 8-bit digital outputs. Although the MIL-Lite analysis software could extract up to 16-bit digital output, it was not practical since the limiting factor of the camera's 8-bit/channel analogue-to-digital converter. The program would artificially pad the digital output from the camera even if output settings were changed to higher resolution. This would make the results unrealistic and unusable for analysis.

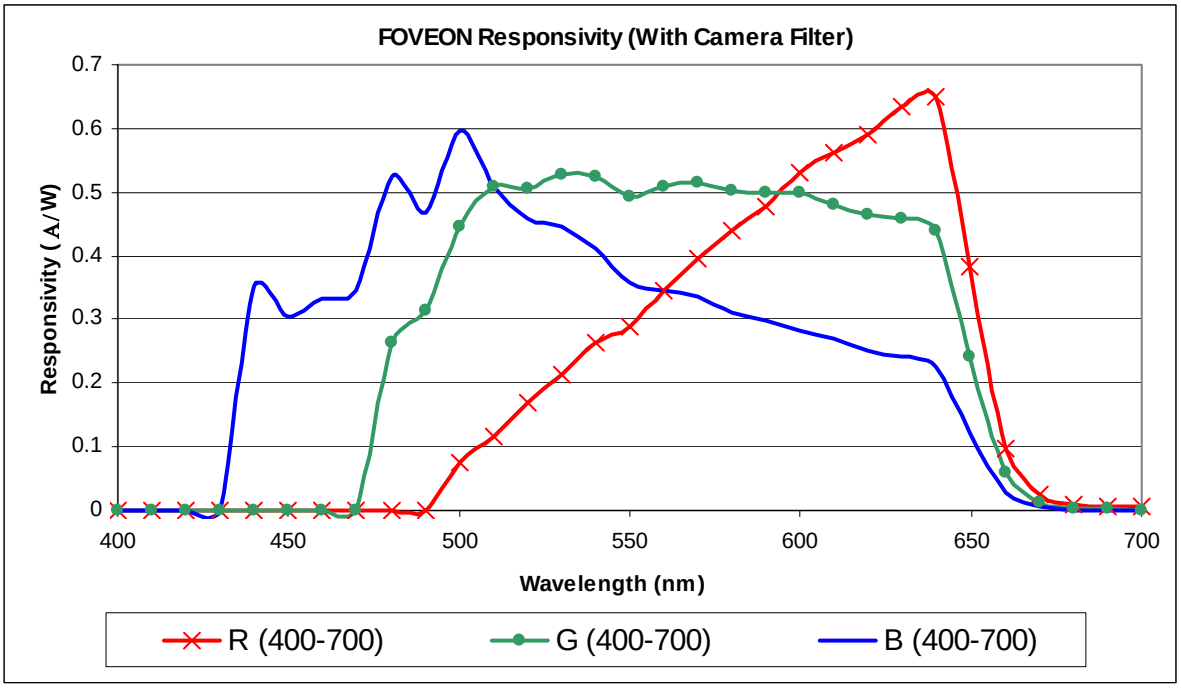

Figure 17. The measured FOVEON responsivity for visible light filtered by the built-in camera filter.

Figure 18 shows the responsivity curves from 600 nm to 1100 nm for light spread over the detector. The curves show two stages of measurement, from 400 nm to 600 nm, and from 600 nm to 1100 nm. The overlap in the responsivity curves for different regions indicates the repeatability in the measurements. The red responsivity above 700 nm demonstrated the FOVEON image sensor's ability to detect near-IR wavelengths. As shown in Figure 16, invisible monochromatic light at 1000 nm wavelength could be imaged.

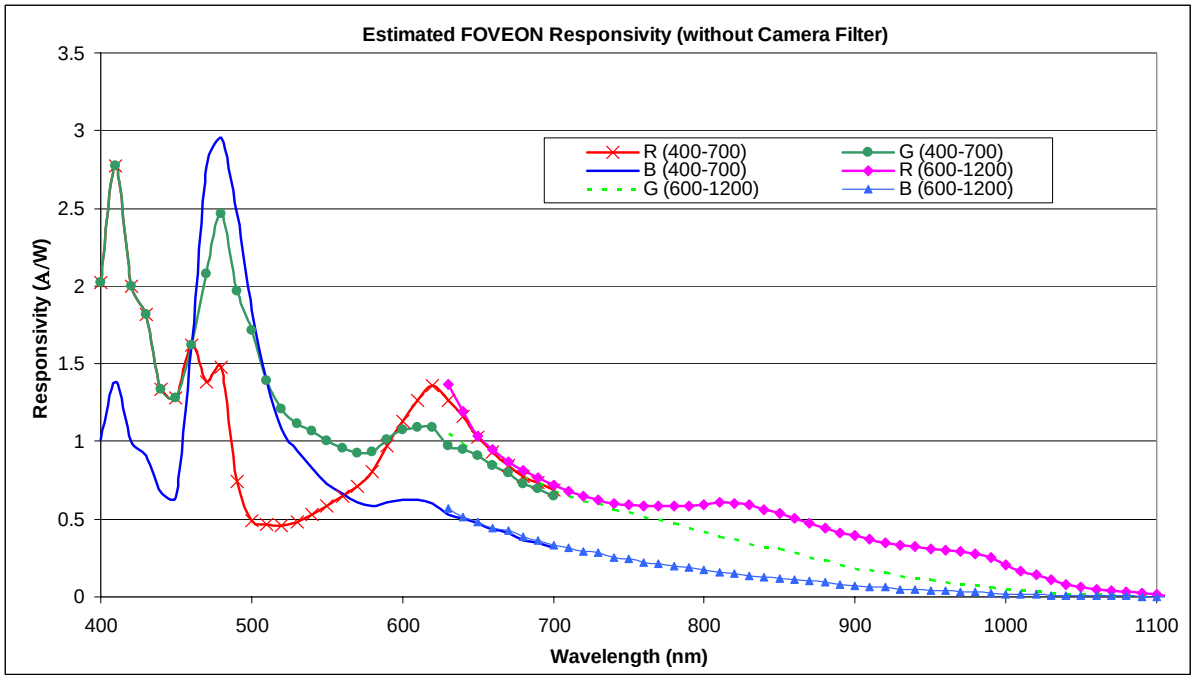

Figure 18. Measured responsivity from 400 nm to 1100 nm showing the signal response in the near-IR wavelengths.

The responsivity curves in the near-UV to blue wavelengths are shown in Figure 19. Although the light was focused on the camera, it was still not bright enough at these wavelengths to provide a sufficiently large signal. To improve the response in the blue signal while suppressing the red and green signals, the Gray Mean Value setting of the camera was adjusted to 250, 250, 20, in the order of red, green and blue input. The Gray Mean Value function was a white balance function allowing the manual adjustment of the color coefficients in the camera. Under different lighting, the same colors will appear differently due the reflectance of the object being imaged. This is also known as metamerism, which will be elaborated in Chapter IV. With suitable input values, the camera can compensate for this effect and produce images with colors that match better to the actual scene. By setting higher levels of a particular primary color and lower input values of another, the camera automatically reduces the signal of output of the color with higher input and increases the color with a lower input value. For example, in the experiments, 250, 250, 20 were chosen as a suitable input for the red, green and blue signals respectively. The camera then reduced the red and green signals while boosting the

blue output. For the near-UV imaging, this worked to increase the very weak blue response and reduce the red and green signals largely caused by noise in the system. Near-UV signals captured in the blue layer were amplified in this manner to produce the image shown in Figure 20.

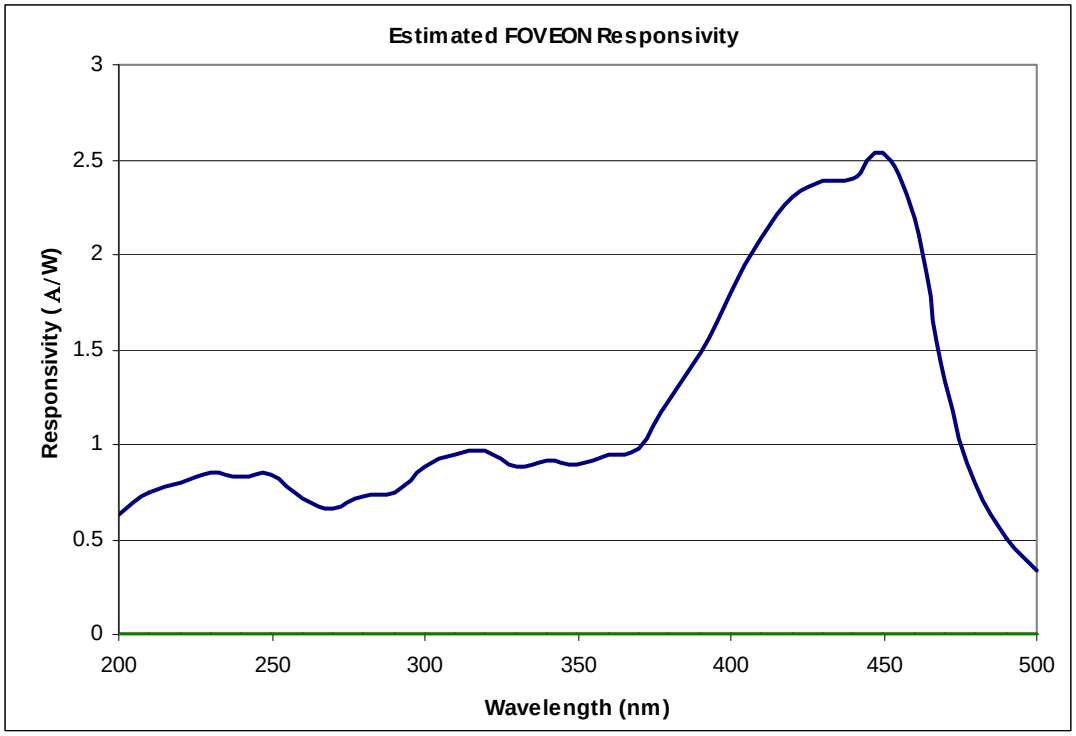

Figure 19. Measured blue responsivity with 250, 250, 20 Gray Mean Value setting enabled.

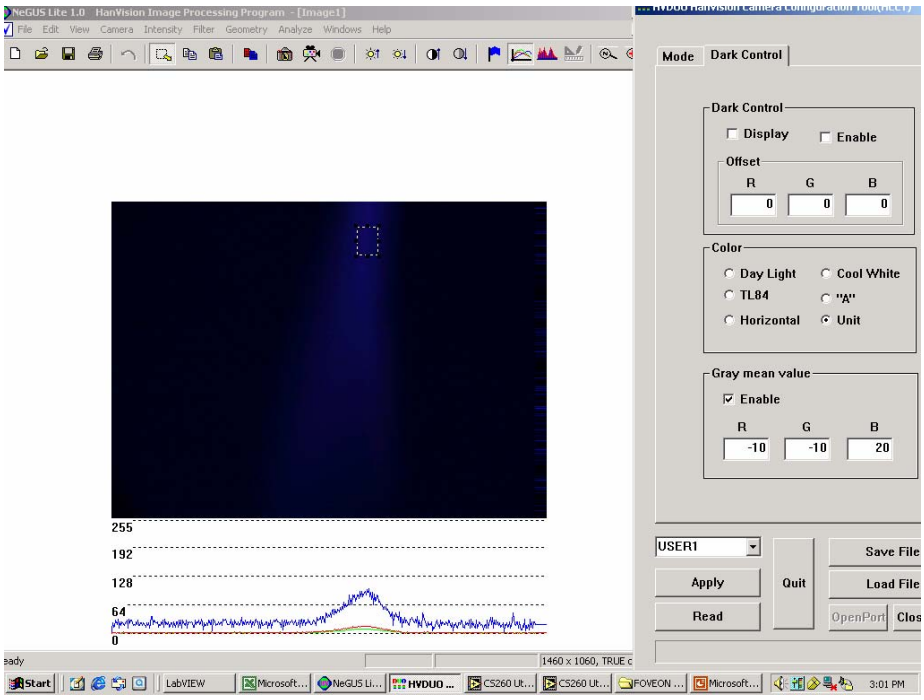

Figure 20. Imaged captured for near-UV light at 200 nm with Gray Mean Value of 250, 250, 20 camera setting. The blue color indicates the detection of near-UV by the "blue" detector.

The relationship between the Gray Mean Value adjustments and the blue output signal was studied for the 250, 250, *x* setting used in the experiment. The red and green inputs were fixed to a value of 250 each while the blue input was increased from a value of 1 to 250. Preliminary results have shown to be non-linear as shown in Figure 21. More experiments are necessary to provide conclusive results, which are beyond the scope of this report. Hence, due to this uncertainty, the near-UV curves were not normalized and plotted with the curves for the visible and near-IR measurements. Nevertheless, the results showed that the Gray Mean Value function could be used as a software gain to image low intensity light at wavelengths below 400 nm.

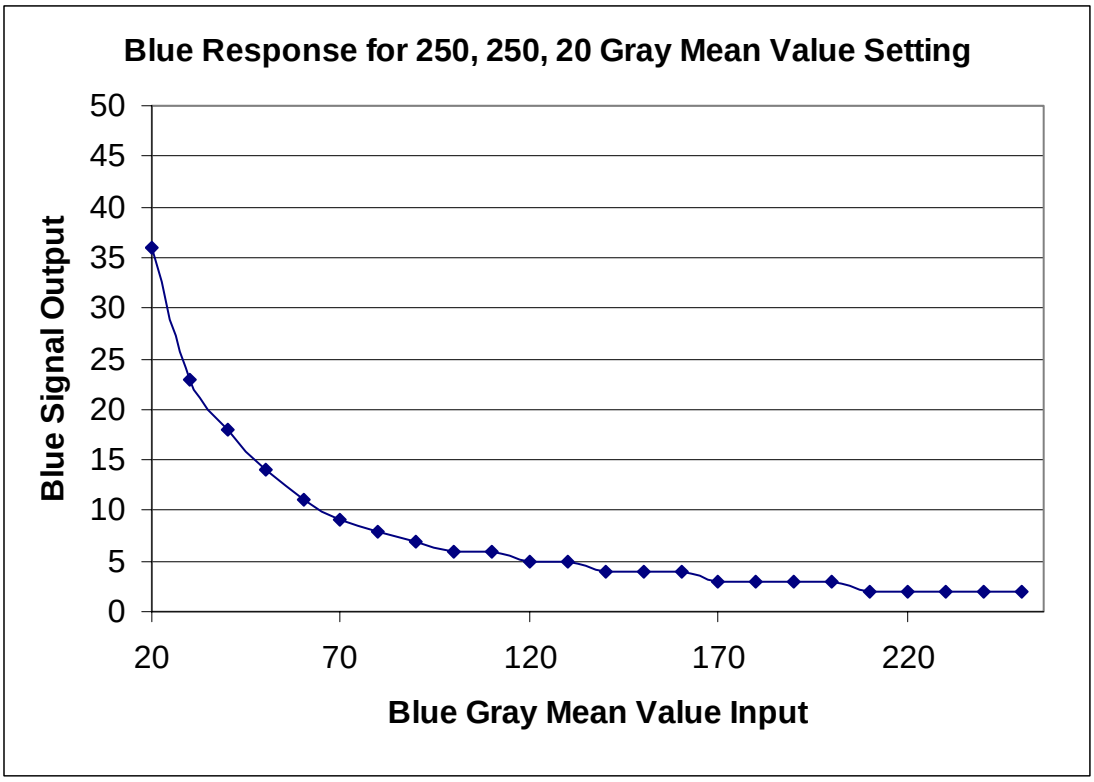

Figure 21. **The relationship between the Gray Mean Value input at 250, 250, x setting and the blue output signal.**

THIS PAGE IS INTENTIONALLY LEFT BLANK.

III. MULTISPECTRAL IMAGING WITH THE FOVEON IMAGE SENSOR

A. GENERAL

Traditional color imaging systems employ photodetector arrays arranged in the Bayer pattern capture images with dedicated blue, green and red detectors. Other sensors such as the Triple Charged Coupled Devices (CCD) systems split the incoming light into the three primary colors before recombination. As illustrated in Figure 4, the FOVEON image sensor is captures images with the same triple-well detector at every pixel location without the need for image interpolation and complex device assembly. However, to produce visible images that are illuminated by non-visible light requires image post-processing. This chapter discusses the theoretical background behind color perception and digital imaging in the HanVision camera as well as some of the outdoor images captured in the near-UV and near-IR wavelengths.

B. NEAR-UV AND NEAR-IR IMAGING

1. Color Perception and Digital Imaging

There are two main image receptors in the human eye. The rod light sensors are extremely sensitive to changes in light levels and are therefore responsible for detecting motion, our peripheral vision and for our ability to see in the dark. They are however, not sensitive to color. The cone sensors on the other hand are sensitive to color and are responsible for our visual acuity. From Kalloniatis and Luu's [13] website, there are three types of cones in our eyes and they detect in the blue (S-cone), green (M-cone) and red (L-cone) wavelengths. They have a range of spectral sensitivities and are represented by tristimulus (or color matching) functions as shown in Figure 22. As presented in Gilblom, Yoo and Ventura's paper on color imaging [4], the goal of imaging systems is to produce images that match these tristimulus curves as closely as possible. This will produce images that are perceived to be most accurately matched to the actual image scene. The FOVEON image sensor and other conventional photodetector arrays employ this concept to

produce images in these three colors, in order for the human nervous system to recognize them.

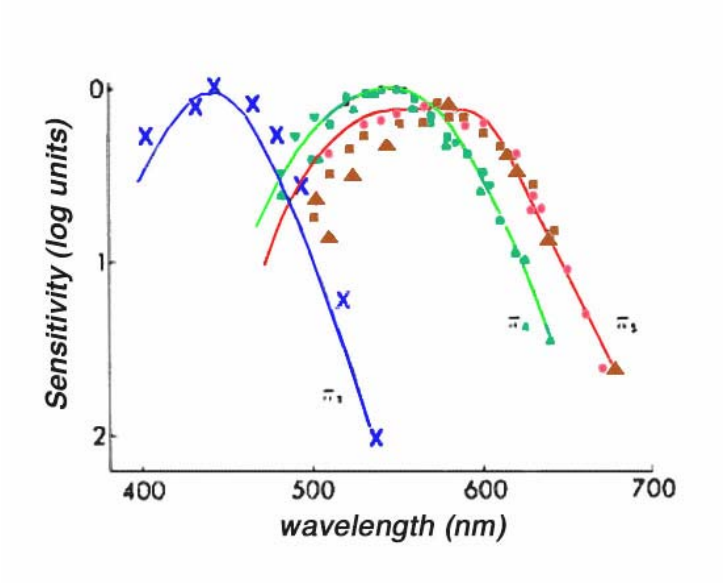

Figure 22. "Spectral sensitivity of the S-cone, M-cone and L-cone. Combined results from various authors using different methods including retinal densitometry from Rushton (green), microspectrometry from Brown and Wald (red) and increment threshold producing artificial monochromasy from Brinley (black) and increment threshold measurements from Wald (X blue) (From Moses, R. S. and Hart, W. M (Ed) Adler's Physiology of the Eye, Clinical Application, St. Louis; The C. V. Mosby Company, 1987)" Extracted from Kalloniatis & Luu [13].

The FOVEON image sensor is a CMOS chip. As shown in Figure 23, photons captured by individual photodetector pixels are converted into voltage signals at the pixel location, unlike CCD detectors [14]. This reduces the data processing requirements within the camera itself. Voltage levels at every pixel in all three layers may also be captured for data processing. As shown in Figure 24, each layer in the FOVEON image sensor captures a specific band of wavelengths. However, longer wavelengths that pass through the upper layers generates signals not only in the intended layer but its upper layers as well. This produces voltage readouts in multiple layers when longer wavelengths are captured. According to the study by Gilblom et al. 0[4], although blue and green responses are produced even when red or near-IR wavelengths are captured, the signals are minimal due to the relatively thin absorption regions in these upper layers.

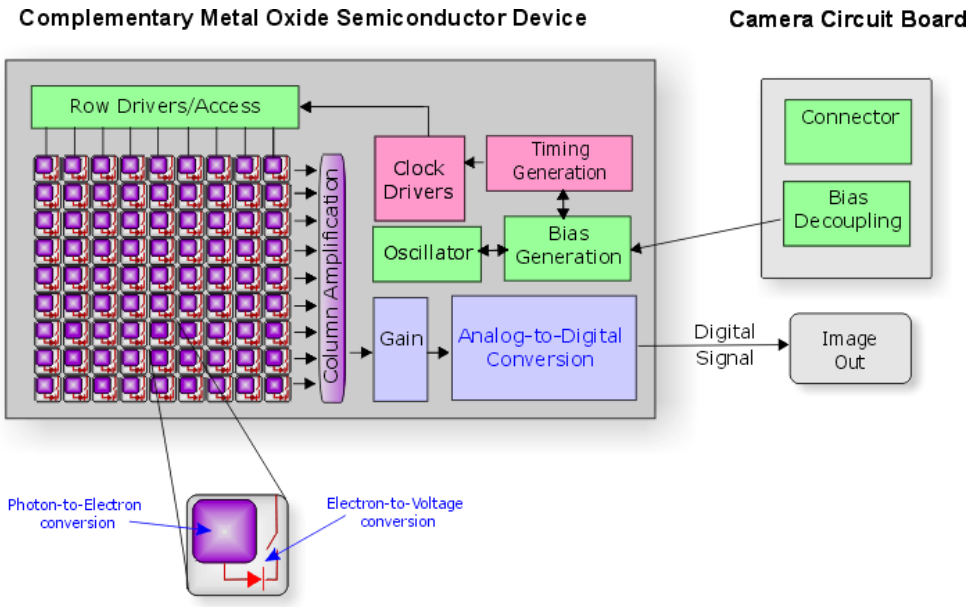

Figure 23. Image Processing within a CMOS Sensor [14].

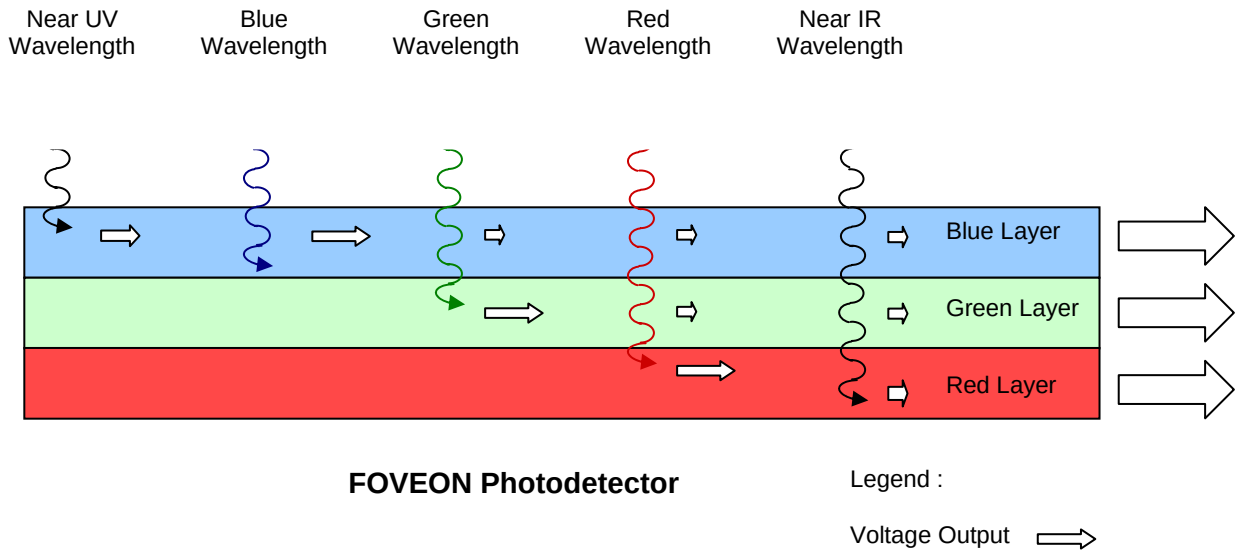

Figure 24. Schematic of FOVEON camera pixel and Absorption Mechanism for the various Wavelengths.

The actual color of the object is obtained by the addition of the three primary colors measured at each of the layers. These values are converted into binary

codes and sent to the PC to be displayed as color images. To adjust the image color for various lighting conditions, various color settings programmed into the camera. These color settings adjust the blue, green and red responses of the image sensor to produce colors that match the image scene as closely as possible. For special applications such as this work, the response settings for all three layers are set to unity and the Gray Mean Value function may be used to manually adjust the white balance of the image. Figure 25 show the block diagram of a HVDUO-10M camera which is almost similar to the HVDUO-5M model used for this thesis. The specifications for both cameras are the same with the exception of lesser dynamic range and a physically smaller detector array installed in the latter model.

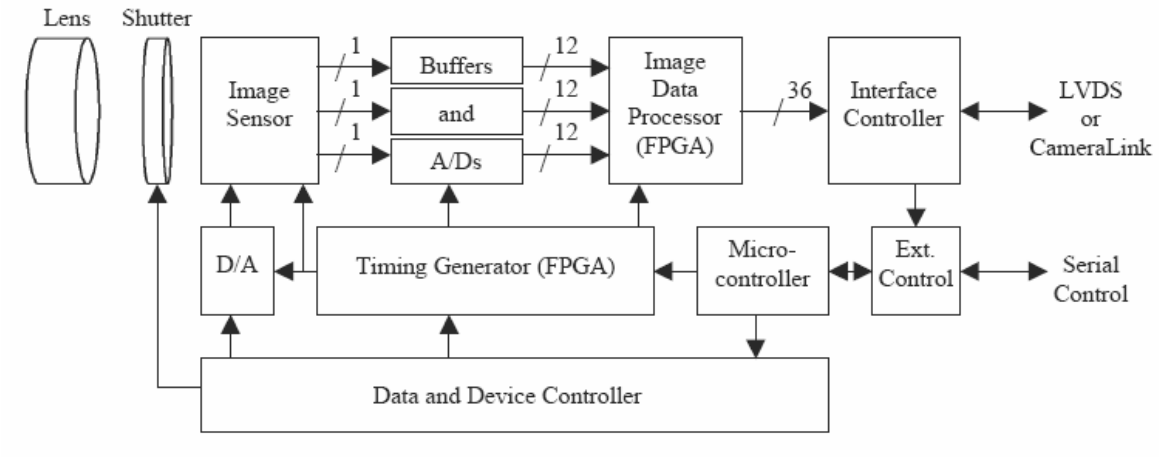

Figure 25. HVDUO-10M Camera Block Diagram (Similar to the HVDUO-5M Camera used for this Thesis) [12].

2. Outdoor Imaging

Numerous outdoor scenes were captured with the HVDUO-5M camera for analysis. The camera set-up consisted of the HVDUO-5M connected to the PC. Images of downtown Monterey and Pacific Grove (Figure 26), approximately 2 km away, were captured from the roof of Spanagel Hall in the Naval Postgraduate School. Other image scenes include the Monterey Bay and passing aircraft arriving and leaving the Monterey Peninsular Airport. An optical filter rack was placed in front of the camera to mount the various filters used in the experiment. The four optical filters used in the experiment were the HOYA U325C, U360, L38 and IR85

filters. The U325C is a UV transmission filter and allows the transmission of wavelengths from approximately 240 nm to 400 nm. It also allows some transmission in the near-IR region from 690 nm to 1100 nm, although this has marginal effect on the captured image. The U360 filter is a narrowband blue pass filter with range from 320 nm to 400 nm. The L38 is a sharp-cut filter allowing the transmission of visible and IR light from 370 nm to 2800 nm. Finally, the IR85 filter allows the transmission of IR light from 850 nm to 2800 nm. Their respective transmission curves were obtained from the HOYA filters company website [ref http://www.hoyafilters.com] and are reproduced in Appendix II of this report.

The effects of various optical filters on the images can be seen in the following sections of this report. The camera was set to "unit" color setting, hence no color compensation was applied to the images. The camera's own filter (400 nm to 660 nm) was removed when the HOYA filters were affixed. As the FOVEON image sensor is able to detect all three colors on a single pixel, the camera is able to have higher image resolution despite having relatively lesser number of pixels (only 1.5 megapixels physically). As shown in Figure 26, the camera is able to capture the image of a car from 2 km away. This achieved by sharpening the image with the NEGUS image analysis software.

Figure 26. Image of downtown Monterey captured with the camera filter (400 nm to 660 nm) affixed. The zoomed-in image of a car is shown.

Due to the unique triple-layered design of the FOVEON detector, it is able to capture near-UV and near-IR photons in the blue and red layers, respectively. A schematic of this concept is shown in Figure 24. This process results in the artificial coloring of light in the near-UV and NIR wavelengths. Near-UV light captured by the camera contributes to the blue signal and appears blue when UV transmitting filters are used. Likewise, near-IR light appears as red as they are captured by in the red layer. In addition, as the long wavelength photons pass through the detector layers to be captured in the red layer, they also produce some signals in the layers above it as well. This is clearly illustrated by the spectral response curves of the camera as shown in Figure 27. These overlapping curves show that the blue and green detection layers show significant response even when wavelengths longer than 550 nm is imaged.

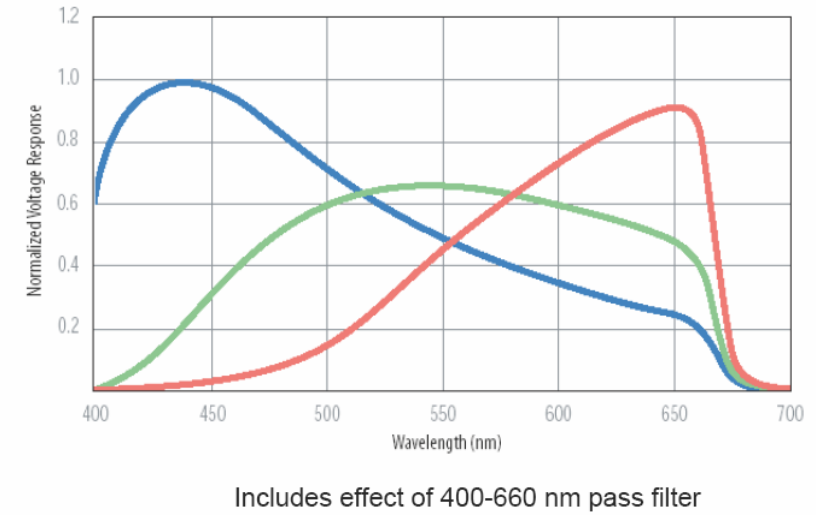

Figure 27. Spectral Response of the FOVEON camera. Each curve represents the response curve of each layer according to its color [12].

The effects of atmospheric absorption as well as the various material reflectances are important in the analysis of the images. Figure 28 shows the absorption characteristics of various molecules in the environment [15]. The white bands indicate the absorption windows of the respective molecules. Near-UV and violet light is absorbed mainly by ozone, nitrogen oxide and atmospheric impurities such as sulfur dioxide. However, near-IR and red wavelengths are strongly

absorbed by water molecules. In Figure 29, the spectral reflectance of various materials was compared [16]. From the graph it can be seen that the man-made construction materials, such as roofing and structural materials, show almost constant reflectance from the near-UV to the near-IR spectrum. The spectral reflectance for the vegetation show strong reflectance in the near-IR wavelengths but lesser reflectance in the near-UV wavelengths, compared to the building materials. These contrasts in reflectance and the effects of molecular absorption allow the discrimination of near-UV and near-IR wavelengths that are captured by the camera. With the UV filter affixed, bright blue colors will indicate a strong UV reflectance whilst faint blue colors will show a strong absorption in UV in that object. Similarly, with the IR filter affixed, bright red colors will indicate strong IR reflectance whilst faint red colors will indicate a very low emission of IR signal.

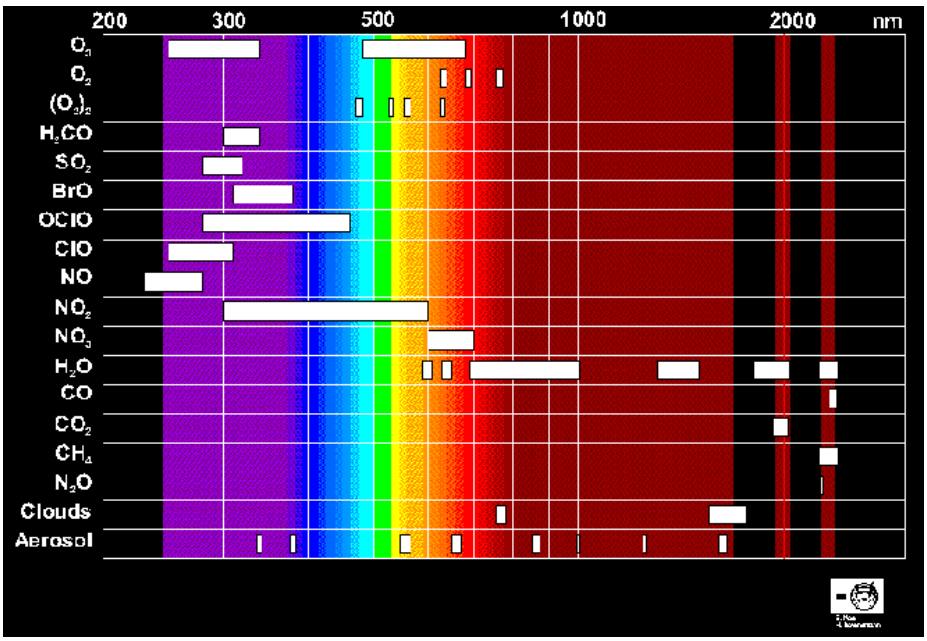

Figure 28. The contribution of the various molecules to atmospheric absorption [15].

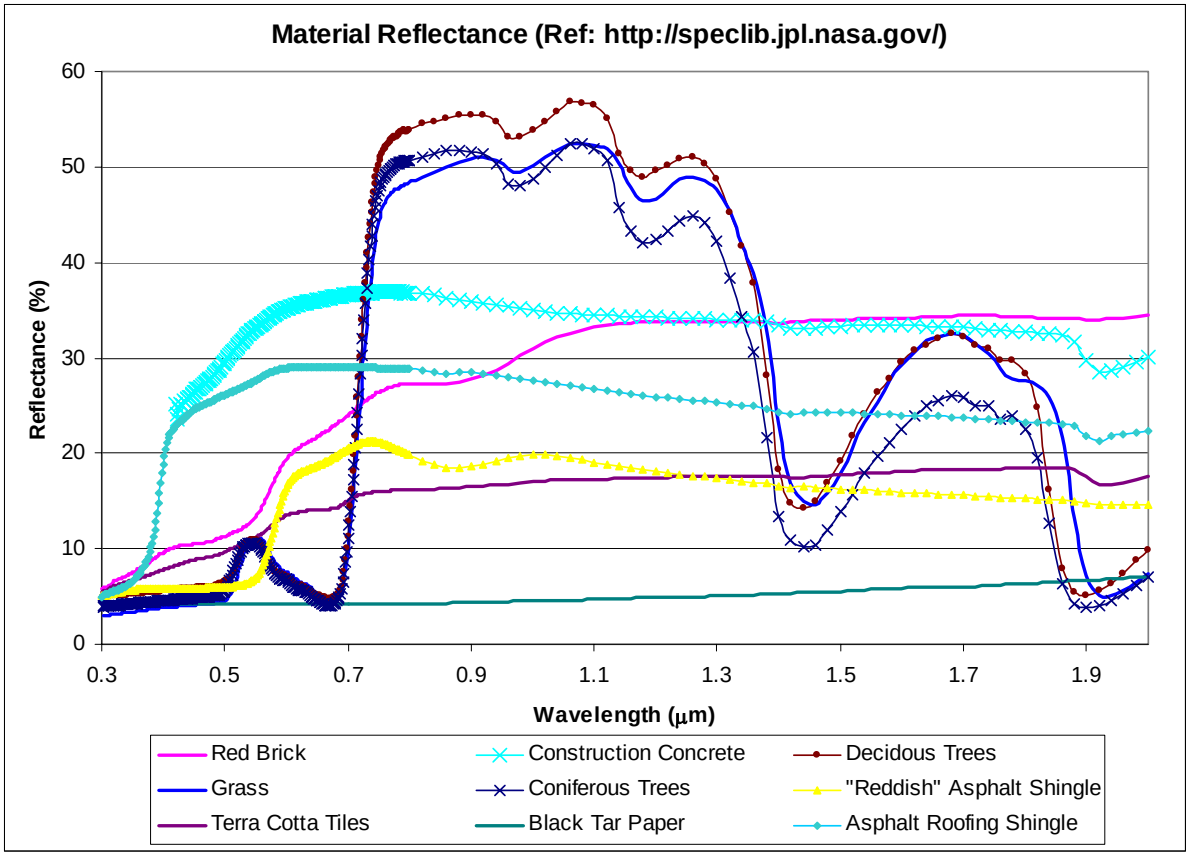

Figure 29. Comparison of the Spectral Reflectance of various Construction Materials and Vegetation [16].

2. Imaging near-UV and near-IR wavelengths

To image in near-UV with the FOVEON camera, it was necessary to affix the U325C filter and to increase the blue response of the camera by adjusting the Gray Mean Value to 250, 250, 20. From the top image in Figure 30, it can be seen that for the same scene as Figure 26, the clouds are more defined and the reflection of UV light from the buildings is contrasted with the surrounding UV absorbing foliage. The reddish tint of the buildings and trees are effects of IR light captured by the camera due to the IR transmitting window of the U325C filter. The blue channel of the same scene is shown below it. In Figure 31, the image captured with the U360 filter show very little spectral information. Compared to the U325C image, the reddish tint in the trees is greatly reduced due to the cut-off in IR transmission. The

contrasts in the clouds, buildings and trees have also been reduced due to the cut-off in near-UV transmission.

Figure 30. Image of downtown Monterey captured with U325C filter (240 nm to 400 nm) (top) and the same scene in its blue channel (bottom).

Figure 31. Image of downtown Monterey captured with U360 filter (320 nm to 400 nm).

With the sun shining from behind the camera, images of Monterey Bay were captured with the U325C and U360 filters. From Figure 32, high near-UV reflection off the surface of the sea can be contrasted with the low near-UV reflection from the buildings and the trees. In addition, sailing boats can be easily distinguished against the color of the sea.

Figure 32. Image of Monterey Bay captured with U325C filter (240 nm to 400 nm).

Near-IR wavelengths were captured with the L38 and IR85 filters. From Figure 33, the L38 filter allows the transmission of both visible and near-IR wavelengths. There is noticeable absence in the blue signal but high IR reflectance from the trees and the houses is clearly visible. From Figure 34, the high contrast between the clouds and the sky can be seen clearly with the IR85 filter. However, compared to the previous figure, there is not much contrast between the houses and the trees due to similar near-IR reflectance from these objects.

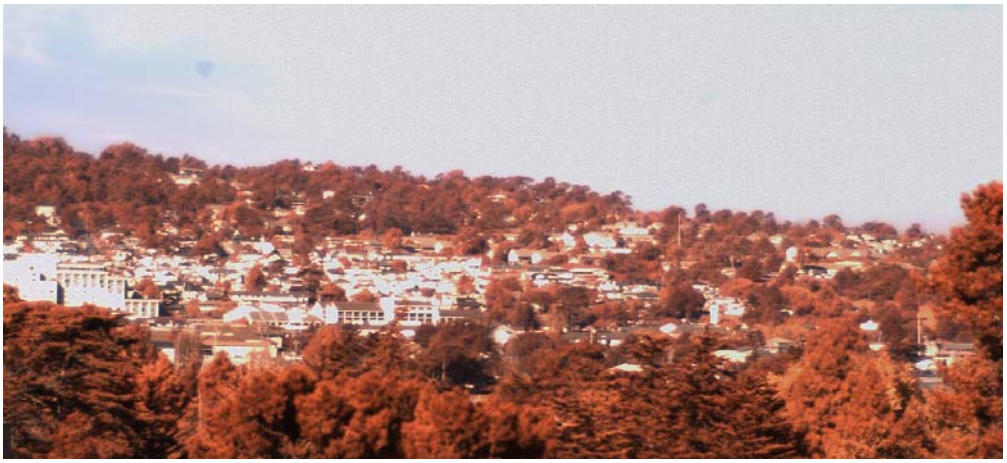

Figure 33. Image of downtown Monterey captured with L38 filter (370 nm to 2800 nm).

Figure 34. Image of downtown Monterey captured with IR85 filter (850 nm to 2800 nm).

Similarly, images of Monterey Bay were also taken with the L38 and IR85 filters. As shown by the image on the left of Figure 35, the IR light can be clearly distinguished from the clouds, as well as from the reflection off the buildings and trees. Similar to the previous figure, there is very little contrast between the buildings and trees. However, the lack of IR reflection off the surface of the sea shows the IR absorption characteristic of sea water. The red channel of the same scene is shown on the right.

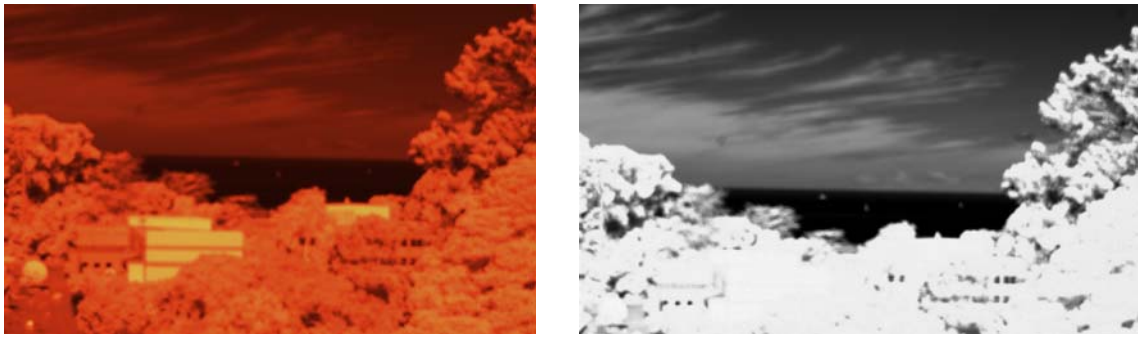

Figure 35. Image of Monterey Bay captured with IR85 filter (850 nm to 2800 nm) (left) and the same scene showing its red channel (right).

Other images including passing aircraft were also imaged with the camera. From Figure 36, the outline of the aircraft as well as the IR reflection off its body can be clearly seen. It was found that the aircraft was difficult to locate in visible light, without the IR filter, even on a clear day. At the same distance from the observer, the aircraft is not well contrasted against the surrounding sky in a visible image. With the IR filter applied, the glare from the sky is greatly reduced providing high contrast between the aircraft and its surroundings. Due to the high resolution of the camera, it is also able to capture very fine image details even in a monochrome color such as red.

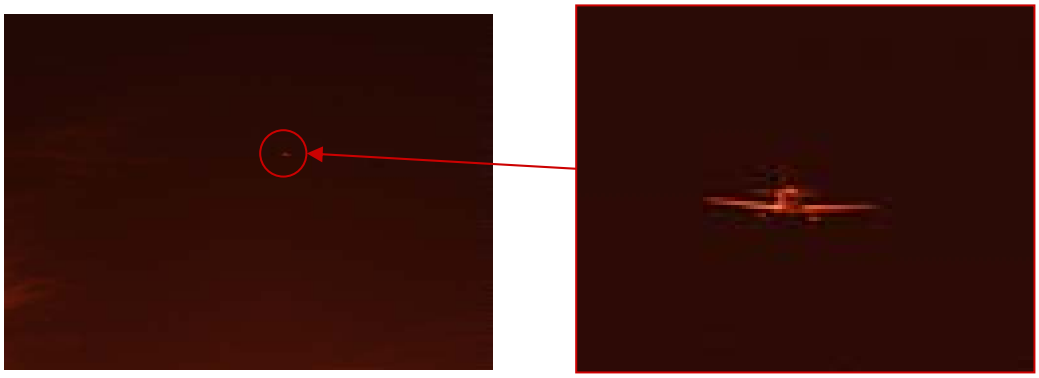

Figure 36. The rear of a passing jet captured with the IR85 filter (850 nm to 2800 nm).

In Figure 37, a camouflage uniform was set up in the midst of some vegetation. With the camera's visible filter (400 nm to 660 nm) on, the scenery looks green and there is not much contrast between the uniform and its surroundings.

Hence even in the day, the shape of the uniform is not easily detected. With the camera filter removed and the UV325C filter on, the image is illuminated more with the sun's UV light and the silhouette of the uniform appears more clearly than the first picture (circled). Figure 38 shows the same scene in its respective red, green and blue channels. Notice that the blue channel gives the best contrast, allowing the uniform to be identified easily.

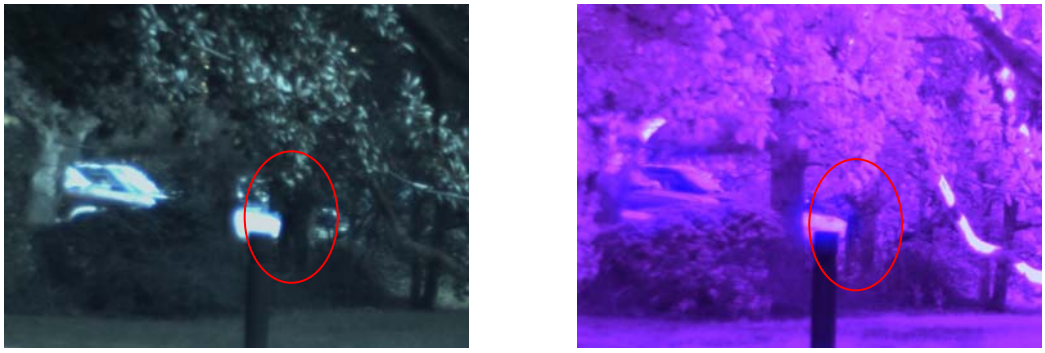

Figure 37. Set-up of a camouflage uniform (circled) in the midst of vegetation showing the image captured in visible light (left) and the UV image (right).

Figure 38. The UV image of the camouflage uniform set-up presented in its respective red (left), green (center) and blue (left) channels. Notice the best contrast is in the blue channel.

THIS PAGE IS INTENTIONALLY LEFT BLANK.

IV. DISCUSSION AND RECOMMENDATIONS

A. NEAR-UV AND NEAR-IR IMAGING

From the discussions and the figures presented in the previous chapter, there are many advantages of the FOVEON camera. Due to its spectral responsivity in the near-UV and near IR wavelengths, it can be easily configured for imaging in these wavelengths using external filters. The detection of UV and IR wavelengths in the blue and red layers of the image sensor allows these wavelengths to be artificially colored. Color coefficients may translate these wavelengths into representative colors, other than red or blue. In addition, the brightness or contrast of the image captured in visible light may be enhanced by the presence of near-UV or near-IR illumination. One of the limitations of employing near-UV and near-IR imaging is in the atmospheric attenuation effects. As shown in Figure 28, molecules and impurities present in the environment may scatter or absorb bands of near-UV and near-IR light. Such interactions reduce the intensity of these wavelengths and limit the effective range of operations. Spectral reflectances of various materials also play a role in contrasting the objects imaged in these wavelengths. However, these features can be used for identification of various objects if the spectral information can be extracted.

Presently, there are many applications that involve the use of near-UV and near-IR wavelengths for imaging. These include defense related applications such as missile seekers designed with solar-blind capabilities. Due to the different reflectance of near-UV light, animal conservationists have also employed near-UV imaging to spot endangered polar bears in the arctic environment that is practically uniform in contrast and color. Forestry departments also employ the use of near-IR imaging to monitor forest fires and de-forestation. The success of these civilian applications may lead to equally successful applications for the military especially in the areas of intelligence operations. With the appropriate optical filters and data processing software, the use of the triple-well image sensor for such purposes may

improve performance. The following section discusses some of these potential applications.

B. FURTHER DEVELOPMENT AND POSSIBILE APPLICATIONS

1. Further Development Possibilities in the Design of Triple-Well Image Sensors

While the FOVEON detector has surpassed conventional digital imaging sensors in performance and has shown that triple-well photodetection may be the next standard in digital imaging, there are a number of potential areas for research. With the advances in material engineering and the better understanding of the human color perception, it is possible to push the boundaries of triple-well photodetector technology even further. In the area of material research, other intrinsic or extrinsic materials may be developed with similar or a greater range of absorption depths. Materials with a greater range of absorption depths may even allow the development of multi-layered photodetectors that are able to capture not just three but more wavelengths including the near-UV and near-IR wavelengths. This development is possible with the growing advancement in semi-conductor manufacturing processes. Similarly, as there are still a number of inconsistencies with the theory of trichromatic vision and its opposing theories [17], it may be worthwhile to develop photodetectors with spectral sensitivities in more wavelength parameters than just the tristimulus curves. An achromatic detector that detects black and white will definitely compliment the imaging performance of the present FOVEON technology very well.

Present studies have proven that the FOVEON detector is able to perform basic imaging in the near-UV and near-IR wavelengths. However, more work is required in the image post-processing stage to convert data captured in these wavelengths into useful and intuitive information for the human operator. In addition, the resolution of the triple-well photodetector needs to be explored both for remote sensing applications as well as microscopy. In a bid to provide higher resolution imaging capabilities, there has been much study into the effects of sensor shape and the arrangement of the various individual detectors. The article by Qi and Synder

[18] quotes that the hexagonal grid pattern requires 13.4% less sampling points to obtain the same high frequency information, and is more efficient than the rectangular grid arrangement currently adopted for the FOVEON image sensor as well as other image sensors arranged in the Bayer Pattern. The same article also states that hexagonal array patterns can model the human visual system more precisely since the cones in the retina are also hexagonal in shape. As the center to center distances between each pixel in the hexagonal array structure are the same, it eliminates the connectivity ambiguity of rectangular grid patterns. In 2000, Fujifilm announced its newest development, the octagonal pixel arrangement pattern, marketed under the trade name “Super CCD” [19]. The company claims that this design, together with its 45-degree alignment system increases sensitivity, improves signal-to-noise ratio and offers a much wider dynamic range.

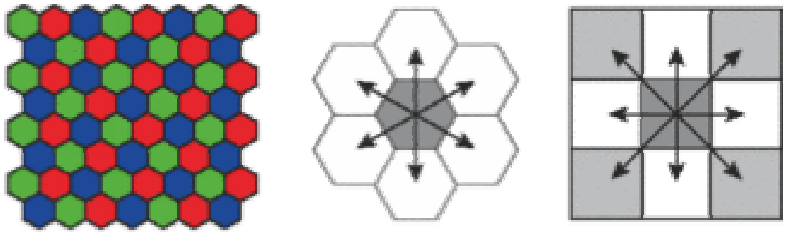

Figure 39. The center to center distances between pixels are constant in a hexagonal arrangement but not in a rectangular pattern [19].

2. Automated Multi-spectral Imaging and Other Applications

As shown from the experiments performed with the FOVEON camera in a combination of both visible and near-UV or near-IR wavelengths, the image obtained has greater brightness and demonstrates higher pixel resolution. In addition, images taken in invisible light reveal other properties of the image scene that may not be perceived by the human eye, such as IR light from hot bodies. From the report by Gilblom et al. [7], it can also be seen the strong UV absorption by certain objects, such as leaves, allow the distinction between natural and man-made items. Hence, sensor systems designed with logic algorithms to recognize signals from these invisible wavelengths may enhance multispectral imaging operations. Other image processing applications include sharpening the captured image in order to

distinguish the finer details before processing the image with edge detection algorithms to provide higher contrast between the subject and the surrounding features. Present multi-spectral imaging techniques also include fusing images captured in different wavelengths together. Some of the potential military applications include the detection of armored vehicles in foliage as well as other counter-camouflage applications. Compared to a Foliage Penetration Radar, a CMOS chip that is able to perform multi-spectral imaging has much potential in man-portable target designation and surveillance operations.

Other areas of potential development for the FOVEON image sensor include improvement in the responsivity especially for near-UV light as well as near-IR imaging for night vision applications.

V. CONCLUSION

While the aim of the thesis was achieved, there were a number of limitations in the thesis research that may be improved for future studies. Due to the time available and the scope of this thesis, it was not able to integrate the camera to other image analysis applications and image capture devices such as laptop framegrabber cards. With the camera operating with laptops, more outdoor sceneries and applications may be explored. In the course of characterizing the camera, it was also found that the dynamic range of the HVDUO-5M was insufficient to provide higher resolution results. The FOVEON image sensor outputs digital signals instead of analog signals due to its CMOS design. For subsequent studies, the use of cameras with larger dynamic range, preferably 10-bits or more per color, would be able to provide better results. As the internal color compensation coefficients of the camera were not know, it was not possible to correlate the effects of the gain settings with the output response in the three colors.

Despite these limitations, this thesis has been successful in conducting a preliminary study in the characteristics and the performance of the FOVEON image sensor. In the course of the research, the Photodetector Characterization System was calibrated and the responsivity of the FOVEON image sensor was measured from 200 nm to 1200 nm. Near-IR and near-UV images were also captured with the aid of various optical filters for image analysis. These images were found to be of high resolution and capable of distinguishing man-made objects from surrounding vegetation when imaged with invisible light. Through the course of the research, a number of topics were explored including the physics behind digital imaging devices as well as the human perception of color. The advantages of the image sensor and areas with potential for further development and applications were also discussed.

There is much potential for triple-well photodetectors as digital imaging devices in the military. Its high spatial and color resolution allows them to be very suitable for intelligence gathering and surveillance applications. The ability to image

near-UV and near-IR wavelengths gives an added edge in the area of multi-spectral imaging. Due to its CMOS construction, it is small in size and cheaper to mass produce than CCDs. This is advantageous in man-portability and large-scale equipping considerations. These are just some of the worthy considerations in favor of triple-well photodetectors replacing conventional photodetectors in both civilian and military applications.

APPENDIX I – UV-035D (S/NO. 7309) CALIBRATION CHART

The following is the calibration chart of the UV-035D UV enhanced photodiode used in the calibration of the Oriel Monochromator.

Wavelength	Responsivity (A/W)	Wavelength	Responsivity (A/W)	Wavelength	Responsivity (A/W)
200	0.07	500	0.242	800	0.418
210	0.078	510	0.25	810	0.423
220	0.084	520	0.256	820	0.429
230	0.09	530	0.262	830	0.435
240	0.094	540	0.268	840	0.44
250	0.089	550	0.275	850	0.445
260	0.082	560	0.281	860	0.45
270	0.076	570	0.288	870	0.455
280	0.078	580	0.294	880	0.46
290	0.087	590	0.3	890	0.464
300	0.099	600	0.305	900	0.472
310	0.106	610	0.31	910	0.477
320	0.11	620	0.315	920	0.481
330	0.113	630	0.322	930	0.486
340	0.115	640	0.329	940	0.491
350	0.101	650	0.334	950	0.494
360	0.102	660	0.34	960	0.499
370	0.104	670	0.346	970	0.499
380	0.114	680	0.351	980	0.501
390	0.131	690	0.357	990	0.496
400	0.147	700	0.361	1000	0.487
410	0.161	710	0.367	1010	0.472
420	0.174	720	0.373	1020	0.447
430	0.185	730	0.379	1030	0.413
440	0.194	740	0.384	1040	0.369
450	0.204	750	0.39	1050	0.318
460	0.212	760	0.396	1060	0.262
470	0.221	770	0.402	1070	0.216
480	0.229	780	0.407	1080	0.18
490	0.236	790	0.412	1090	0.149
				1100	0.121

Table 4. Responsivity Values of Calibrated UV-035D Photodiode (S/N 7309).

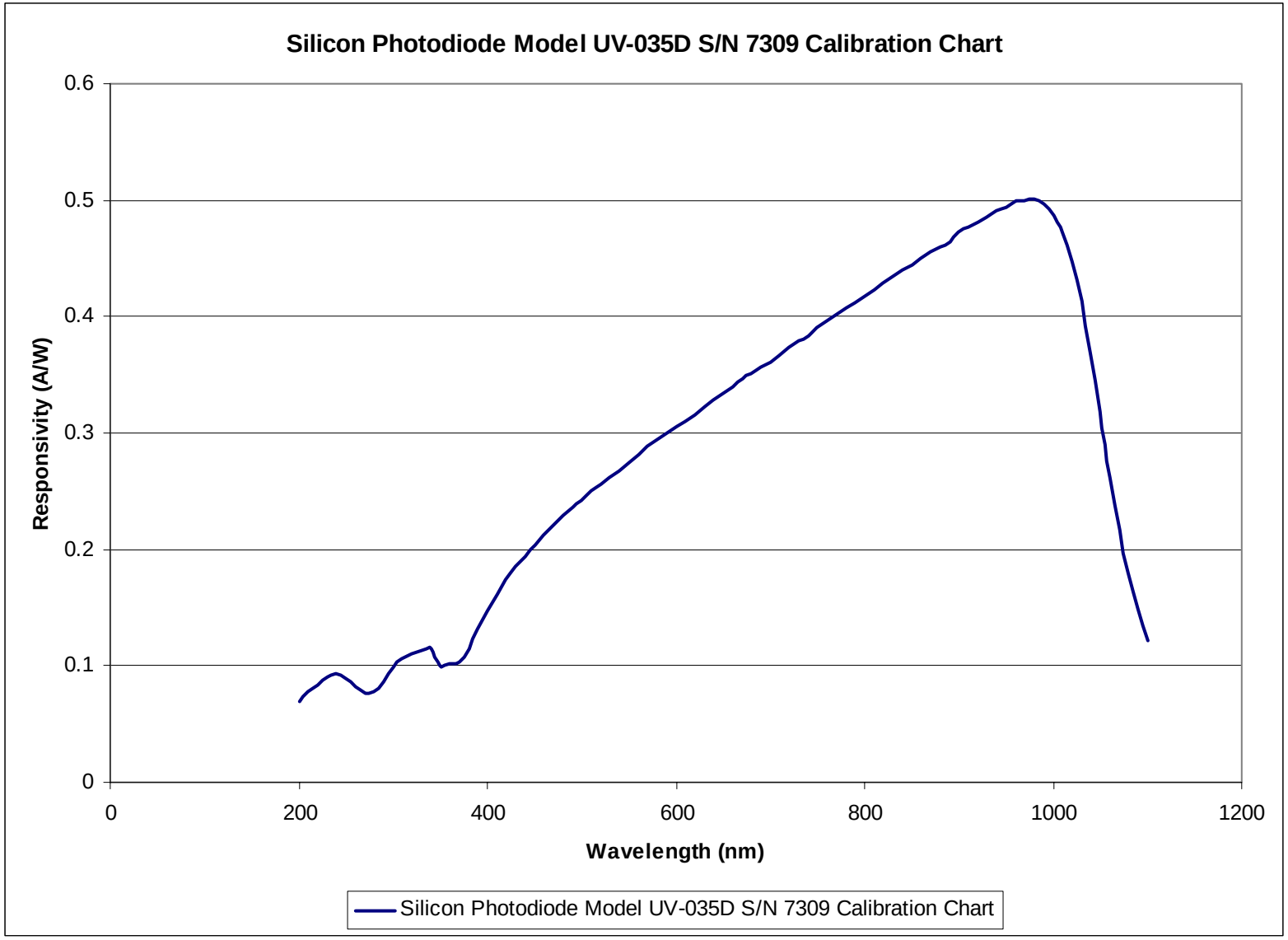

Figure 40. Calibrated Responsivity Chart of the UV-035D Photodiode (S/N 7309).

APPENDIX II – TRANSMISSION CURVES OF HOYA FILTERS

The following are the transmission curves of the HOYA filters used in the research. They are all reproduced from the HOYA filters website available on the world wide web at www.hoyafilters.com.

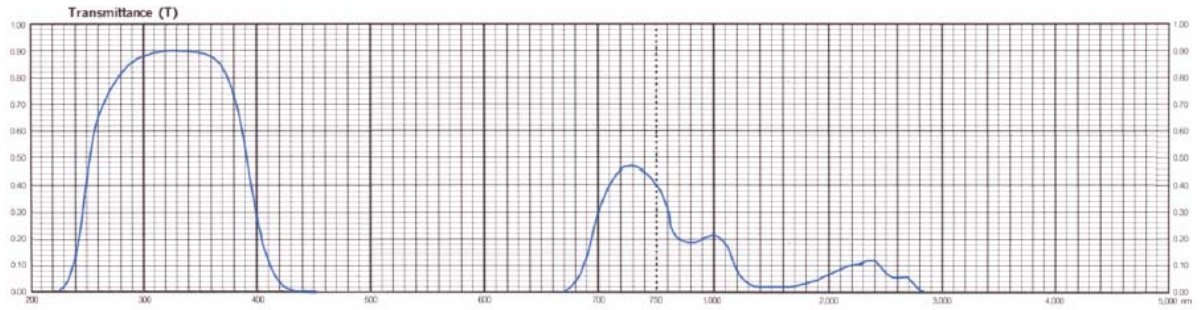

Figure 41. Transmission curve of HOYA U325C filter.

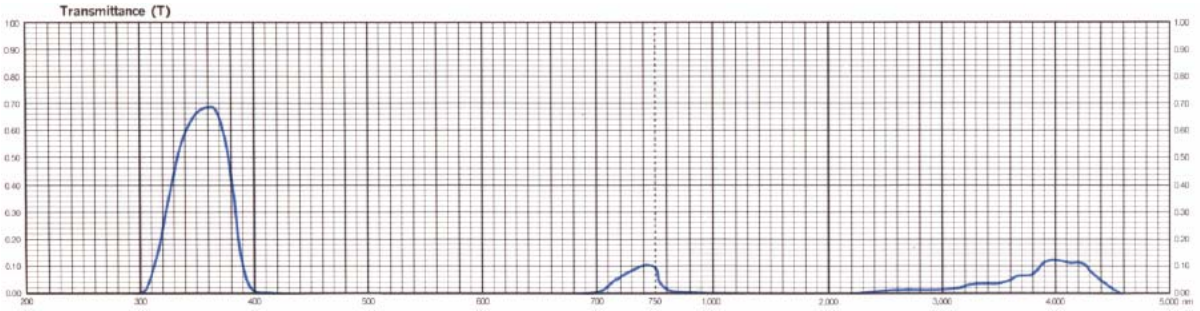

Figure 42. Transmission curve of HOYA U360 filter.

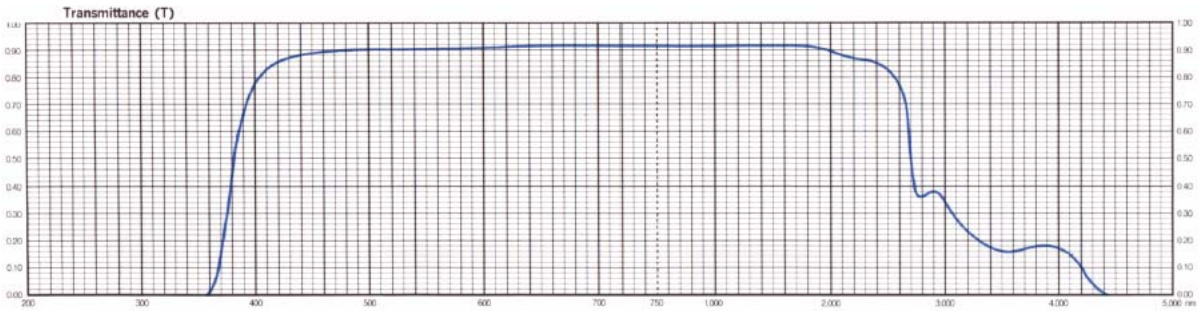

Figure 43. Transmission curve of HOYA L38 filter.

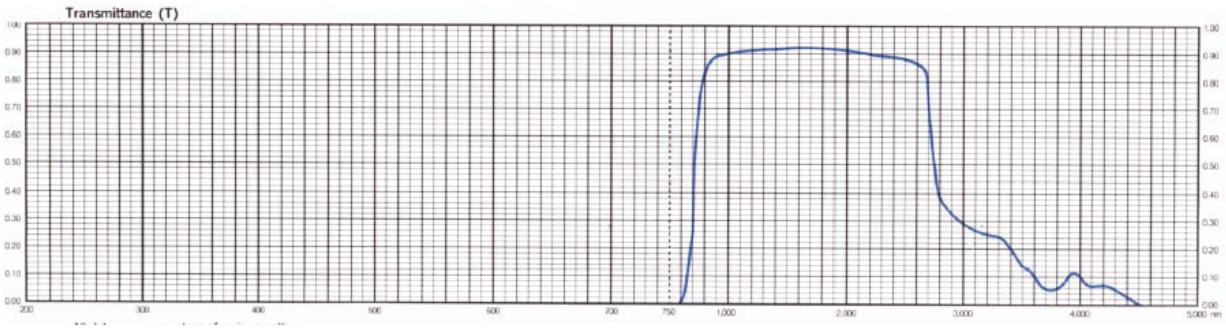

Figure 44. Transmission curve of HOYA IR85 filter.

LIST OF REFERENCES

[1] FOVEON Inc. (2004) *FOVEON - Why X3 is Better*; available from World Wide Web @http://www.foveon.com/X3_better.html, cited Jul 2004.

[2] Rogers, A. (1997) *Essentials of Optoelectronics with Applications*, London: Chapman and Hall.

[3] Merrill, R. B. *Color Separation in an Active Pixel Cell Imaging Array Using a Triple-Well Structure*, United States Patent No. 5965875, Oct 12 1999.

[4] Gilblom, D. L., Yoo, S.K. & Ventura, P. (2003) *Operation and Performance of a Color Image Sensor with Layered Photodiodes*, SPIE, Vol. 5074; available from World Wide Wed @http://www.alt-vision.com/documents/5074-35.pdf, cited Aug 2004.

[5] Tomkins, M. R. *FOVEON: New CMOS sensor captures triple the data (2002)*;available from World Wide Web @http://www.imaging-resource.com/EVENTS/PMAS02/1013470528.html, cited Nov 2004.

[6] Hynes, S. *The X Factor*, Professional Photographer Feb 2003 Pg 59-63; available from World Wide Web @www.totaldp.com/articles_download.cfm?action=download_sample&id=54&site=PP&sh=1&mh=50, cited Nov 2004.

[7] Gilblom, D. L. & Yoo, S. K. (2004) *Infrared and Ultraviolet Imaging with a CMOS Sensor having Layered Photodiodes*, SPIE/ISA Electronic Imaging 2004; available from World Wide Web @http://www.alt-vision.com/documents/5301A-25.pdf, cited Aug 2004.

[8] HanVision Co. Ltd. *HVDUO-5M Digital Camera with FOVEON X3 Direct Color Image Sensor*, Product Brochure; available from World Wide Web @http://www.hanvision.com/index.html?PFiPack_Session=fc7a016623208a47d15997d5cdd5b361, cited Sep 2004.

[9] Herdlick, B. E. (2002) *Computer-Controlled Photodetector Characterization System (Design and Construction)*, Naval Postgraduate School MSc Thesis, Dec 2002.

[10] UDT Sensors Inc. *UV Enhanced Series – Inversion Layers and Planar Diffused Silicon Photodiodes*, Product Brochure; available from World Wide Web @http://www.udt.com/Datasheets/Products/UVEnhancedSeries.pdf, cited Jul 2004.

[11] HanVision Co. Ltd (2004) *HCCT User Guide*.

[12] Gilblom, D. L., Yoo, S. K. & Ventura, P. (2003) *Real-time Color Imaging with a CMOS Sensor having Stacked Photodiodes*, SPIE Annual Meeting 2003; available from World Wide Web @http://www.alt-vision.com/documents/5210-14.PDF, cited Aug 2004.

[13] Kalloniatis, M. & Luu, C. *Psycho Physics of Vision*; available from World Wide Web @http://webvision.med.utah.edu/KallColor.html#overview, cited Oct 2004.

[14] Technical Advisory Service for Images (TASI) (2003) *Advice Paper – Digital Cameras*; available from World Wide Web @http://www.tasi.ac.uk/advice/creating/pdf/camera.pdf, cited Oct 2004.

[15] ESA (2004) *Atmospheric Absorption*; available from World Wide Web @http://envisat.esa.int/support-docs/atmospheric-absorption/atmospheric-absorption.html, cited Nov 2004.

[16] NASA Jet Propulsion Laboratory (2002) *ASTER Spectral Library*; available from World Wide Web @http://speclib.jpl.nasa.gov, cited Nov 2004.

[17] Encyclopædia Britannica (2004) *Colour* . Encyclopædia Britannica Premium Service; available from World Wide Web @ http://www.britannica.com/eb/article?tocId=21866, cited Oct 2004.

[18] Qi, H. & Snyder, W. E. (2004) *Infrared Imaging Learns from Camera Industry*, Laser Focus World, July 2004.

[19] Fujifilm (2004) *News Highlights – New 4th Generation Super CCD Producing higher resolution and wider dynamic range by sophisticated miniaturization technologies*, Fujifilm website; available from World Wide Web @ http://home.fujifilm.com/news/n030122.html, cited Oct 2004.

[20] Technical Advisory Service for Images (TASI) (2004) *Advice Paper – Colour Theory: Understanding and Modelling Colour*; available from World Wide Web @http://www.tasi.ac.uk/advice/creating/pdf/colour.pdf, cited Oct 2004.

[21] Nave, R. (2000) *Color Perception*, Hyperphysics website, Georgia State University; available from World Wide Web @http://hyperphysics.phy-astr.gsu.edu/hbase/vision/colper.html#c1, cited Oct 2004.

[22] Poynton, C. (1997) *Frequently Asked Questions about Color*; available from World Wide Web @ http://www.poynton.com/PDFs/ColorFAQ.pdf, cited Oct 2004.

[23] Technical Advisory Service for Images (TASI) (2004) *Advice Paper – Colour Management in Practice*; available from World Wide Web @http://www.tasi.ac.uk/advice/creating/pdf/colour2.pdf, cited Oct 2004.

[24] Scott, E. & Bewley, H. (1997) *Color Vision – Human Perception of Different Wavelengths of Light*; available from World Wide Web @http://www.photo.net/photo/edscott/vis00010.htm, cited Oct 2004.

[25] HunterLab (1997) *Application Notes – Metamerism Index*; available from World Wide Web @http://www.hunterlab.com/appnotes/an03_97.pdf, cited Oct 2004.

[26] HunterLab (2000) *Application Notes – Color Inconsistency*; available from World Wide Web @http://www.hunterlab.com/appnotes/an11_00.pdf, cited Oct 2004.

[27] H Cho Ed. (2003) *Opto-Mechatronic Systems Handbook – Techniques and Applications*, CRC Press.

[28] Matrox Electronic Systems Ltd. (2000) *Matrox Intellicam ver 2.07- User Guide*.

[29] Lyon, R. F. & Hubel, P. M. *Eyeing the Camera: Into the Next Century*, IS&T/SID Tenth Color Imaging Conference; available from World Wide Web @http://www.foveon.com/docs/Century.pdf, cited Aug 2004.

INITIAL DISTRIBUTION LIST

1. Defense Technical Information Center
   Fort Belvoir, Virginia

2. Dudley Knox Library
   Naval Postgraduate School
   Monterey, CA

3. Professor Gamani Karunsiri
   Naval Postgraduate School
   Monterey, CA

4. Professor Richard Christopher Olsen
   Naval Postgraduate School
   Monterey, CA

5. Professor James Luscombe
   Naval Postgraduate School
   Monterey, CA